

Low-Complexity Variable Forgetting Factor Mechanism for Blind Adaptive Constrained Constant Modulus Algorithms

Yunlong Cai, Rodrigo C. de Lamare, Minjian Zhao and Jie Zhong

Abstract

In this work, we propose a novel low-complexity variable forgetting factor (VFF) mechanism for blind adaptive constrained constant modulus (CCM) recursive least squares (RLS) algorithms applied to linear interference suppression in direct-sequence code-division multiple access (DS-CDMA) systems. The proposed variable forgetting factor mechanism employs an updated component related to the time average of the constant modulus (CM) cost function to automatically adjust the forgetting factor in order to ensure good tracking of the interference and the channel. Convergence and tracking analyses are carried out. Analytical expressions for predicting the mean-squared error of the proposed adaptation technique are obtained. Simulation results are presented for nonstationary environments and show that the proposed variable forgetting factor mechanism achieves superior performance to previously reported methods at a reduced complexity.

Index Terms— Blind multiuser detection, adaptive filtering, variable forgetting factor mechanisms.

I. INTRODUCTION

Blind interference suppression techniques with adaptive implementation have attracted considerable interest and found applications in beamforming, multiuser detection, source separation and radar systems [1]-[18]. They operate without knowledge of the channel input, and lead to a solution comparable to that obtained from the minimization of the mean squared error (MSE) [1], [5]. The constrained minimum variance (CMV) based algorithms are designed in such a way that they attempt to minimize the filter output power while maintaining a constant response in the

Y. Cai, M. Zhao and J. Zhong are with Department of Information Science and Electronic Engineering, Zhejiang University, Hangzhou 310027, China (e-mail: ylcai@zju.edu.cn, mjzhao@zju.edu.cn, zhongjie@zju.edu.cn).

R. C. de Lamare is with the Communications Research Group, Department of Electronics, University of York, YO10 5DD York, U.K. (e-mail: rcdl500@ohm.york.ac.uk).

This work is supported by the Fundamental Research Funds for the Central Universities and the NSF of China under Grant 61101103.

direction of a signal of interest [1]-[6]. In [1], the authors have investigated the adaptive blind CMV receiver for direct-sequence code-division multiple access (DS-CDMA) systems in additive white Gaussian noise (AWGN) channels, and have presented an analysis of the algorithm. The blind CMV receiver has been extended to multipath fading channels in [2]. A novel variable step-size mechanism for CMV stochastic gradient (SG) algorithms has been proposed in [3]. The work in [4] has developed a CMV beamforming algorithm using the Kalman Filter for multiuser cooperative relay networks. A reduced-rank strategy based on the joint and iterative optimization (JIO) of a subspace projection matrix and a reduced-rank filter has been reported in [5] for beamforming, whereas algorithms with switching mechanisms have been considered in [6] for airborne radar systems. A drawback of CMV-based algorithms is that they are sensitive to mismatches and imperfections.

The constrained constant modulus (CCM) based algorithms are based on a criterion that penalizes deviations of the modulus of the received signal away from a fixed value and forced to satisfy one or a set of linear constraints such that signals from the desired user are detected [13], [15]. In particular, the work in [13] and [15] has demonstrated the robustness of the blind adaptive techniques with the CCM criterion against nonstationary environments, which can be implemented with a SG or a recursive least squares (RLS) algorithm. The works in [7], [8] have considered standard SG algorithms with fixed step sizes to implement the blind CCM receiver. Some previous works have shown significant gains in performance due to the use of averaging methods [9], [10]. The authors in [11], [12], [13] have proposed some variable step-size schemes to accelerate the convergence speed of the CCM-SG filters, where one SG algorithm adapts the parameter vector and another SG recursion adapts the step-size. The work of [14] has developed the blind CCM algorithm with adaptive RLS implementation in multipath fading channels. Two novel reduced-rank techniques based on the blind CCM receivers have been recently proposed in [15], [16]. In addition, blind adaptive interference suppression techniques have also been developed for use with decision feedback receivers in DS-CDMA systems [17], [18].

The RLS algorithm is considered as one of the fastest and most effective methods for adaptive implementation [26]. However, in nonstationary wireless environments in which users often enter and exit the system, it is impractical to compute a predetermined value for the forgetting factor. Furthermore, there is a very small number of works employing variable forgetting factor (VFF) mechanisms and, to the best of our knowledge, there has been no work with blind variable forgetting factor techniques using the constant modulus (CM) criterion. The most common method is the gradient-based variable forgetting factor (GVFF) algorithm proposed in [26], where a GVFF scheme with the MSE criterion is investigated. In this work, we propose a novel low-complexity variable forgetting factor mechanism for blind linear receivers for DS-CDMA systems using the CCM criterion and RLS algorithms. The proposed variable forgetting factor mechanism employs an updated component related to the time average of the CM cost function to automatically adjust the forgetting factor in order to ensure good tracking of the interference and

the channel. We refer to the proposed variable forgetting factor scheme as time-averaged variable forgetting factor (TAVFF). Convergence and tracking analyses of the proposed adaptation technique are carried out and analytical expressions to predict the MSE are obtained. Simulation results are presented for nonstationary environments, showing that the new mechanism achieves superior performance to previously reported methods at a reduced complexity. The main contributions of this paper are summarized as follows:

- I) A low-complexity variable forgetting factor mechanism combined with blind CCM-RLS receivers is introduced for multipath DS-CDMA channels.
- II) We extend the conventional GVFF mechanism to blind adaptive algorithms with the CM criterion.
- III) The convergence and tracking analyses of the adaptive CCM-RLS receiver with the proposed TAVFF mechanism are carried out. We derive formulas to predict the steady-state MSE and analyze the complexity of the blind GVFF and proposed TAVFF mechanisms.
- IV) We perform a simulation study of the proposed and existing techniques.

The paper is structured as follows. Section II briefly describes the system model and the design of linearly constrained receivers. The adaptive blind CCM-RLS algorithm and the blind GVFF scheme are introduced in section III. The proposed TAVFF mechanism and its steady-state analysis are described in section IV. Convergence and tracking analyses of the resulting algorithm and the analytical formulas to predict the steady-state MSE are developed in section V. The simulation results are presented in section VI. Finally, section VII draws the conclusions. Below, we give a summary defining the abbreviations used in the paper to improve its readability.

- VFF: variable forgetting factor.
- CCM: constrained constant modulus.
- RLS: recursive least squares.
- DS-CDMA: direct-sequence code-division multiple access.
- CM: constant modulus.
- MSE: mean squared error.
- CMV: constrained minimum variance.
- AWGN: additive white Gaussian noise.
- SG: stochastic gradient.
- JIO: joint and iterative optimization.
- GVFF: gradient-based variable forgetting factor.
- TAVFF: time-averaged variable forgetting factor.
- BPSK: binary phase-shift keying.
- MIMO: multi-input multi-output.

- OFDM: orthogonal frequency-division multiplexing.
- FIR: finite impulse response.
- LMS: least mean square.
- SINR: signal-to-interference-plus-noise ratio.
- BER: bit error rate.
- SNR: signal-to-noise ratio.
- ISI: intersymbol interference.

II. DS-CDMA SYSTEM MODEL AND DESIGN OF LINEARLY CONSTRAINED RECEIVERS

Let us consider the downlink of an uncoded synchronous binary phase-shift keying (BPSK) DS-CDMA system with K users, N chips per symbol and L_p propagation paths. A synchronous model is assumed for simplicity since it captures most of the features of more realistic asynchronous models with small to moderate delay spreads. Let us assume that the signal has been demodulated at the mobile user, the channel is constant during each symbol and the receiver is perfectly synchronized with the main channel path. The received signal after filtering by a chip-pulse matched filter and sampled at chip rate yields an M -dimensional received vector at time i

$$\mathbf{r}(i) = \sum_{k=1}^K (A_k b_k(i) \mathbf{C}_k \mathbf{h}(i) + \boldsymbol{\eta}_k(i)) + \mathbf{n}(i), \quad (1)$$

where $M = N + L_p - 1$, $\mathbf{n}(i) = [n_1(i) \dots n_M(i)]^T$ is the complex Gaussian noise vector with zero mean and $E[\mathbf{n}(i)\mathbf{n}^H(i)] = \sigma^2 \mathbf{I}$ whose components are independent and identically distributed, where $(\cdot)^T$ and $(\cdot)^H$ denote transpose and Hermitian transpose, respectively, and $E[\cdot]$ stands for expected value. The user symbols are denoted by $b_k(i)$, where we assume that the symbols are independent and identically distributed random variables with equal probability from the set $\{\pm 1\}$. The amplitude of user k is A_k , and the signature of user k is represented by $\mathbf{p}_k = [a_k(1) \dots a_k(N)]^T$. The $M \times L_p$ constraint matrix \mathbf{C}_k that contains one-chip shifted versions of the signature sequence for user k and the $L_p \times 1$ vector $\mathbf{h}(i)$ with the multipath components are described by

$$\mathbf{C}_k = \begin{bmatrix} a_k(1) & & \mathbf{0} \\ \vdots & \ddots & a_k(1) \\ a_k(N) & & \vdots \\ \mathbf{0} & \ddots & a_k(N) \end{bmatrix}, \mathbf{h}(i) = \begin{bmatrix} h_0(i) \\ \vdots \\ h_{L_p-1}(i) \end{bmatrix}, \quad (2)$$

where the $M \times 1$ vector $\mathbf{C}_k \mathbf{h}(i)$ denotes the effective spreading code. The vector $\boldsymbol{\eta}_k(i)$ denotes the intersymbol interference (ISI) for user k , here we express the ISI vector in a general form that is given by $\boldsymbol{\eta}_k(i) = A_k b_k(i-1) \mathbf{H}^p \mathbf{p}_k + A_k b_k(i+1) \mathbf{H}^s \mathbf{p}_k$, where the $M \times N$ matrices \mathbf{H}^p and \mathbf{H}^s account for the ISI from previous and

subsequent symbols, respectively, and can be given as follows

$$\mathbf{H}^p = \begin{bmatrix} 0 & \dots & h_{L_p-1}(i-1) & \dots & h_1(i-1) \\ 0 & & \ddots & & \vdots \\ \vdots & & & h_{L_p-1}(i-1) & \\ 0 & & & \vdots & \\ 0 & 0 & \dots & 0 & 0 \end{bmatrix}, \mathbf{H}^s = \begin{bmatrix} 0 & 0 & \dots & 0 & 0 \\ \vdots & & & & 0 \\ h_0(i+1) & & & & \vdots \\ \vdots & & \ddots & & 0 \\ h_{L_p-2}(i+1) & \dots & h_0(i+1) & \dots & 0 \end{bmatrix}. \quad (3)$$

The linear model in (1) can be used to represent other wireless communications systems including multi-input multi-output (MIMO) and orthogonal frequency-division multiplexing (OFDM) systems. For example, the user signatures of a DS-CDMA system are equivalent to the spatial signatures of a MIMO system.

The CCM linear receiver design is equivalent to determining a finite impulse response (FIR) filter $\mathbf{w}_k(i)$ with M coefficients that provide an estimate of the desired symbol as follows

$$z_k(i) = \mathbf{w}_k^H(i)\mathbf{r}(i), \quad (4)$$

where the detected symbol is given by $\hat{b}_k(i) = \text{sign}\{\Re[\mathbf{w}_k^H(i)\mathbf{r}(i)]\}$, where the operator $\Re[\cdot]$ retains the real part of the argument and $\text{sign}\{\cdot\}$ is the signum function.

The design of the receive filter $\mathbf{w}_k(i)$ is based on the optimization of the CM cost function

$$\bar{J}_{CM}(\mathbf{w}_k(i)) = E\left[(|\mathbf{w}_k^H(i)\mathbf{r}(i)|^2 - 1)^2 \right] \quad (5)$$

subject to the constraints given by $\mathbf{w}_k^H(i)\mathbf{C}_k\mathbf{h}(i) = \nu$, where ν is a constant to ensure the convexity of the optimization problem as discussed in [14]. The CCM receive filter expression that iteratively solves the constrained optimization problem in (5) is given by

$$\mathbf{w}_k(i+1) = \bar{\mathbf{Q}}_k^{-1}(i) \left(\bar{\mathbf{d}}_k(i) - \left(\mathbf{h}^H(i)\mathbf{C}_k^H\bar{\mathbf{Q}}_k^{-1}(i)\mathbf{C}_k\mathbf{h}(i) \right)^{-1} \left(\mathbf{h}^H(i)\mathbf{C}_k^H\bar{\mathbf{Q}}_k^{-1}(i)\bar{\mathbf{d}}_k(i) - \nu \right) \mathbf{C}_k\mathbf{h}(i) \right), \quad (6)$$

where $i = 1, 2, \dots$ and $\bar{\mathbf{Q}}_k(i) = E[|z_k(i)|^2\mathbf{r}(i)\mathbf{r}^H(i)]$, $\bar{\mathbf{d}}_k(i) = E[z_k^*(i)\mathbf{r}(i)]$, $z_k(i) = \mathbf{w}_k^H(i)\mathbf{r}(i)$. A detailed derivation of the CCM estimation approach can be found in [14], [15], [16]. It should be remarked that the expression in (6) is a function of previous values of the filter $\mathbf{w}_k(i)$ and therefore must be iterated in order to reach a solution. The CCM design can have its convexity enforced by adjusting the parameter ν [14], [5]. Thus, we obtain the optimum CCM receiver for a given channel $\mathbf{h}(i)$ as follows

$$\mathbf{w}_0 = \bar{\mathbf{Q}}_0^{-1} \left(\bar{\mathbf{d}}_0 - \left(\mathbf{h}^H(i)\mathbf{C}_k^H\bar{\mathbf{Q}}_0^{-1}\mathbf{C}_k\mathbf{h}(i) \right)^{-1} \left(\mathbf{h}^H(i)\mathbf{C}_k^H\bar{\mathbf{Q}}_0^{-1}\bar{\mathbf{d}}_0 - \nu \right) \mathbf{C}_k\mathbf{h}(i) \right), \quad (7)$$

where $\bar{\mathbf{Q}}_0 = E[|z_0(i)|^2\mathbf{r}(i)\mathbf{r}^H(i)]$, $\bar{\mathbf{d}}_0 = E[z_0^*(i)\mathbf{r}(i)]$, $z_0(i) = \mathbf{w}_0^H\mathbf{r}(i)$ and \mathbf{w}_0 denotes the optimum CCM receiver. In addition to this, the iterative method in (6) assumes the knowledge of the channel parameters. Since there is a large number of applications that have to deal with unknown multipath propagation, it is also important to be able to blindly estimate the multipath components.

In order to blindly estimate the channel, a designer can adopt the blind channel estimation procedure based on the subspace approach reported in [2], [30] and which is described by

$$\hat{\mathbf{h}}(i) = \arg \min_{\mathbf{h}(i)} \mathbf{h}^H(i) \mathbf{C}_k^H \mathbf{R}^{-1}(i) \mathbf{C}_k \mathbf{h}(i) \quad (8)$$

subject to $\|\mathbf{h}(i)\| = 1$, where $\mathbf{R}(i) = E[\mathbf{r}(i)\mathbf{r}^H(i)]$. The solution is the eigenvector of the $L_p \times L_p$ matrix corresponding to the minimum eigenvalue of $\mathbf{C}_k^H \mathbf{R}^{-1}(i) \mathbf{C}_k$ through eigenvalue decomposition.

III. BLIND ADAPTIVE CCM-RLS ALGORITHMS AND PROBLEM STATEMENT

In this section, we describe the multipath blind adaptive CCM-RLS algorithm for estimating the parameters of the linear receiver first, and then we generalize the blind GVFF scheme [26] for the multipath adaptive CCM-RLS receiver.

A. Multipath Blind Adaptive CCM-RLS Algorithm

Consider the time-averaged cost function $J_{CM}(i) = \sum_{n=1}^i \gamma^{i-n} (|\mathbf{w}_k^H(i)\mathbf{r}(n)|^2 - 1)^2$ subject to the constraint $\mathbf{w}_k^H(i)\mathbf{C}_k\mathbf{h}(i) = \nu$, where γ denotes the forgetting factor. Given $\mathbf{h}(i)$, we take into account the unconstrained optimization problem given in the form of a Lagrangian cost function

$$J'_{CM}(i) = \sum_{n=1}^i \gamma^{i-n} (|\mathbf{w}_k^H(i)\mathbf{r}(n)|^2 - 1)^2 + \lambda(\mathbf{w}_k^H(i)\mathbf{C}_k\mathbf{h}(i) - \nu) + \lambda^*(\mathbf{h}^H(i)\mathbf{C}_k^H\mathbf{w}_k(i) - \nu), \quad (9)$$

where λ denotes the Lagrangian multiplier. By taking the gradient of (9) with respect to $\mathbf{w}_k^*(i)$ and setting it to zero, after further mathematical manipulations we have

$$\mathbf{w}_k(i) = \mathbf{Q}_k^{-1}(i) \left(\mathbf{d}_k(i) - \frac{\lambda}{2} \mathbf{C}_k \mathbf{h}(i) \right) \quad (10)$$

where $\mathbf{Q}_k(i) = \sum_{n=1}^i \gamma^{i-n} |\mathbf{w}_k^H(i)\mathbf{r}(n)|^2 \mathbf{r}(n)\mathbf{r}^H(n)$ and $\mathbf{d}_k(i) = \sum_{n=1}^i \gamma^{i-n} \mathbf{r}(n)\mathbf{r}^H(n)\mathbf{w}_k(i)$. By multiplying $\mathbf{h}^H(i)\mathbf{C}_k^H$ on the left side of (10), and using $\mathbf{h}^H(i)\mathbf{C}_k^H\mathbf{w}_k(i) = \nu$, we have

$$\lambda = 2(\mathbf{h}^H(i)\mathbf{C}_k^H\mathbf{Q}_k^{-1}(i)\mathbf{C}_k\mathbf{h}(i))^{-1}(\mathbf{h}^H(i)\mathbf{C}_k^H\mathbf{Q}_k^{-1}(i)\mathbf{d}_k(i) - \nu). \quad (11)$$

By substituting (11) into (10) we obtain

$$\mathbf{w}_k(i) = \mathbf{Q}_k^{-1}(i) \left(\mathbf{d}_k(i) - (\mathbf{h}^H(i)\mathbf{C}_k^H\mathbf{Q}_k^{-1}(i)\mathbf{C}_k\mathbf{h}(i))^{-1}(\mathbf{h}^H(i)\mathbf{C}_k^H\mathbf{Q}_k^{-1}(i)\mathbf{d}_k(i)\mathbf{C}_k\mathbf{h}(i) - \nu\mathbf{C}_k\mathbf{h}(i)) \right). \quad (12)$$

Letting $\mathbf{u}_k(i) = z_k(i)\mathbf{r}(i)$ and employing the matrix inversion lemma and Kalman RLS recursions [26], we have the following expressions

$$\mathbf{s}_k(i) = \frac{\mathbf{Q}_k^{-1}(i-1)\mathbf{u}_k(i)}{\gamma + \mathbf{u}_k^H(i)\mathbf{Q}_k^{-1}(i-1)\mathbf{u}_k(i)} \quad (13)$$

$$\mathbf{Q}_k^{-1}(i) = \gamma^{-1}\mathbf{Q}_k^{-1}(i-1) - \gamma^{-1}\mathbf{s}_k(i)\mathbf{u}_k^H(i)\mathbf{Q}_k^{-1}(i-1) \quad (14)$$

$$\mathbf{d}_k(i) = \gamma \mathbf{d}_k(i-1) + z_k^*(i) \mathbf{r}(i). \quad (15)$$

The CCM-RLS algorithm is given by (12)-(15). The problem we are interested in solving is how to devise a cost-effective mechanism to adjust γ , which is a key factor affecting the performance of CCM-RLS-based algorithms.

B. Blind GVFF Scheme in Multipath Channels

To adjust the forgetting factor automatically, let us extend the GVFF scheme in [26] to the adaptive CCM-RLS algorithm in multipath CDMA channels. By taking the gradient of the instantaneous CM cost function $(|\mathbf{w}_k^H(i)\mathbf{r}(i)|^2 - 1)^2$ with respect to the variable forgetting factor $\gamma(i)$ we obtain the following adaptive rule

$$\gamma(i+1) = \left[\gamma(i) - \mu \frac{\partial((|\mathbf{w}_k^H(i)\mathbf{r}(i)|^2 - 1)^2)}{\partial \gamma} \right]_{\gamma^-}^{\gamma^+}, \quad (16)$$

where

$$\frac{\partial((|\mathbf{w}_k^H(i)\mathbf{r}(i)|^2 - 1)^2)}{\partial \gamma} = (|\mathbf{w}_k^H(i)\mathbf{r}(i)|^2 - 1) \Re[\mathbf{Y}_k^H(i)\mathbf{r}(i)\mathbf{r}^H(i)\mathbf{w}_k(i)], \quad (17)$$

and $\mathbf{Y}_k(i)$ denotes an $M \times 1$ vector which is given by $\mathbf{Y}_k(i) = \frac{\partial \mathbf{w}_k(i)}{\partial \gamma}$, $[.]_{\gamma^-}^{\gamma^+}$ denotes the truncation to the limits of the range $[\gamma^-, \gamma^+]$, μ denotes a small, positive step-size. According to [26], the upper level of truncation, γ^+ , plays a relatively insignificant role, we can set it equal to a positive value which is less than but close to 1. The lower level of truncation, γ^- that ensures the stability plays a more important role and should be determined by simulations. Setting a too small value for γ^- may cause the algorithm to become unstable. The updated equation of $\mathbf{Y}_k(i)$ can be obtained by taking the gradient of (12) with respect to $\gamma(i)$. Thus, we generate two new quantities $\frac{\partial \mathbf{Q}_k^{-1}(i)}{\partial \gamma}$ and $\frac{\partial \mathbf{d}_k(i)}{\partial \gamma}$, updated equations of which can be obtained by following the same approach using (14) and (15). Note that we generate another new quantity $\frac{\partial \mathbf{s}_k(i)}{\partial \gamma}$ by computing $\frac{\partial \mathbf{Q}_k^{-1}(i)}{\partial \gamma}$. The updated equation of $\frac{\partial \mathbf{s}_k(i)}{\partial \gamma}$ can be similarly obtained by differentiating (13). For the details of the expressions, see (68), (69), (70) and (71) in the appendix. The CCM-RLS receiver with the GVFF mechanism is implemented by using (12)-(16) and the updated equations of $\mathbf{Y}_k(i)$, $\frac{\partial \mathbf{Q}_k^{-1}(i)}{\partial \gamma}$, $\frac{\partial \mathbf{d}_k(i)}{\partial \gamma}$ and $\frac{\partial \mathbf{s}_k(i)}{\partial \gamma}$ with initial values.

IV. PROPOSED TAVFF SCHEME

In this section, we first introduce the proposed low-complexity variable forgetting factor scheme that adjusts the forgetting factor of the adaptive CCM-RLS algorithm. Then, a steady-state analysis of the proposed variable forgetting factor scheme is carried out. Finally, we present the computational complexity analysis for the proposed TAVFF mechanism and the blind GVFF mechanism.

A. Blind TAVFF Mechanism

Motivated by the variable step-size mechanism for least mean square (LMS) algorithms in [23], we have devised the following time-averaged expression

$$\phi(i) = \delta_1\phi(i-1) + \delta_2(|\mathbf{w}_k^H(i)\mathbf{r}(i)|^2 - 1)^2, \quad (18)$$

where $\phi(i)$ denotes an updated component that is controlled by the instantaneous CM cost function, $0 < \delta_1 < 1$, and $\delta_2 > 0$. The updated component $\phi(i)$ is a small value, and it changes rapidly as the instantaneous value of the cost function [23], [13]. The use of $\phi(i)$ has the potential to provide a suitable indication of the evolution of the cost function. Thus, unlike the blind GVFF mechanism we aim to design a simpler mechanism that adjusts the forgetting factor automatically based on $\phi(i)$. Note that the forgetting factor should vary in an inversely proportional way to the value of the cost function, we have experimented a number of rules and the following expression is a result of several attempts to devise a simple and yet effective mechanism

$$\gamma(i) = \left[\frac{1}{1 + \phi(i)} \right]_{\gamma^-}^{\gamma^+}. \quad (19)$$

The proposed low-complexity TAVFF mechanism is given by (18) and (19). The value of variable forgetting factor $\gamma(i)$ is close to 1, and it is controlled by the parameters δ_1 and δ_2 . Normally, δ_1 is close to 1, and δ_2 is set equal to a small value. A large prediction error will cause the updated component $\phi(i)$ to increase, which simultaneously reduces the forgetting factor $\gamma(i)$ and provides a faster tracking. While a small prediction error will result in a decrease in the updated component $\phi(i)$, thereby the forgetting factor $\gamma(i)$ is increased to yield a smaller misadjustment.

We first show the convergence and derive the expressions for the steady-state statistical properties of the updated component $\phi(i)$. Since $0 < \delta_1 < 1$, by taking the expectation of (18) we can see that $E[\phi(i)]$ converges. According to [22], [7] and [24], we assume $\lim_{i \rightarrow \infty} E[(|\mathbf{w}_k^H(i)\mathbf{r}(i)|^2 - 1)^2] = \xi_{min} + \xi_{ex}(\infty)$, where we have $\xi_{min} = 3|\mathbf{w}_0^H\mathbf{R}(i)\mathbf{w}_0|^2 - 2\mathbf{w}_0^H\mathbf{R}(i)\mathbf{w}_0 - 2\|\mathbf{w}_0^H\bar{\mathbf{C}}\|_4^4 + 1$, $\bar{\mathbf{C}} = [A_1\mathbf{C}_1\mathbf{h}, A_2\mathbf{C}_2\mathbf{h}, \dots, A_K\mathbf{C}_K\mathbf{h}, A_1\mathbf{H}^p\mathbf{p}_1, \dots, A_K\mathbf{H}^p\mathbf{p}_K, A_1\mathbf{H}^s\mathbf{p}_1, \dots, A_K\mathbf{H}^s\mathbf{p}_K]$, $\|\mathbf{x}\|_4$ denotes the 4-norm computation defined by $\sqrt[4]{\sum_i |x_i|^4}$, and $\xi_{ex}(\infty)$ denotes the steady-state excess error of the CM cost function, $\xi_{min} \gg \xi_{ex}(\infty)$ [22]. We obtain

$$E[\phi(\infty)] \approx \frac{\delta_2(\xi_{min} + \xi_{ex}(\infty))}{1 - \delta_1} \approx \frac{\delta_2\xi_{min}}{1 - \delta_1}. \quad (20)$$

Using (18), by computing the square of $\phi(i)$ we obtain

$$\begin{aligned} \phi^2(i) &= \delta_1^2\phi^2(i-1) + 2\delta_1\delta_2\phi(i-1)(|\mathbf{w}_k^H(i)\mathbf{r}(i)|^2 - 1)^2 + \delta_2^2(|\mathbf{w}_k^H(i)\mathbf{r}(i)|^2 - 1)^4 \\ &\approx \delta_1^2\phi^2(i-1) + 2\delta_1\delta_2\phi(i-1)(|\mathbf{w}_k^H(i)\mathbf{r}(i)|^2 - 1)^2, \end{aligned} \quad (21)$$

where we neglect the last term since δ_2^2 is sufficiently small. By taking the expectation we have

$$E[\phi^2(i)] \approx \delta_1^2E[\phi^2(i-1)] + 2\delta_1\delta_2E[\phi(i-1)]E[(|\mathbf{w}_k^H(i)\mathbf{r}(i)|^2 - 1)^2], \quad (22)$$

where when $i \rightarrow \infty$, we assume that $\phi(i-1)$ and $(|\mathbf{w}_k^H(i)\mathbf{r}(i)|^2 - 1)^2$ are uncorrelated,

$$E[\phi(i-1)(|\mathbf{w}_k^H(i)\mathbf{r}(i)|^2 - 1)^2] \approx E[\phi(i-1)]E[(|\mathbf{w}_k^H(i)\mathbf{r}(i)|^2 - 1)^2], \quad (23)$$

the proof is given in the Appendix. Due to the fact that $0 < \delta_1^2 < 1$, we can see that $E[\phi^2(i)]$ converges. When $i \rightarrow \infty$, we obtain

$$E[\phi^2(\infty)] \approx \frac{2\delta_1\delta_2^2(\xi_{min} + \xi_{ex}(\infty))^2}{(1-\delta_1^2)(1-\delta_1)} \approx \frac{2\delta_1\delta_2^2\xi_{min}^2}{(1-\delta_1^2)(1-\delta_1)}, \quad (24)$$

where we assume $(\xi_{min} + \xi_{ex}(\infty))^2 \approx \xi_{min}^2$, since $\xi_{min} \gg \xi_{ex}(\infty)$.

Let us derive the steady-state first order and second order statistical properties for the variable forgetting factor. From (18) and (21) we can see that the quantities $\phi(i)$ and $\phi^2(i)$ are small values, and $\phi(i)$ and $\phi^2(i)$ vary slowly around their mean values, respectively. Thus, using (19), when $i \rightarrow \infty$ we have

$$E[\gamma(\infty)] \approx \frac{1}{1 + E[\phi(\infty)]}. \quad (25)$$

By squaring (19) and following the approximation, we have

$$E[\gamma^2(\infty)] \approx \frac{1}{1 + 2E[\phi(\infty)] + E[\phi^2(\infty)]}. \quad (26)$$

By substituting (20) and (24) into (25) and (26), respectively, we have the steady-state statistical properties for the variable forgetting factor

$$E[\gamma(\infty)] \approx \frac{1 - \delta_1}{1 + \delta_2\xi_{min} - \delta_1}, \quad (27)$$

and

$$E[\gamma^2(\infty)] \approx \frac{(1 - \delta_1)^2(1 + \delta_1)}{(1 - \delta_1)^2(1 + \delta_1) + 2\delta_2(1 - \delta_1)(1 + \delta_1)\xi_{min} + 2\delta_1\delta_2\xi_{min}^2}. \quad (28)$$

B. Computational Complexity

We study the computational complexity of the CCM-RLS algorithm with the proposed TAVFF mechanism in DS-CDMA systems. In Table I, we compute the number of additions and multiplications to compare the complexity of the CCM-RLS algorithm with the TAVFF mechanism and the CCM-RLS algorithm with the conventional blind GVFF mechanism. In particular, for a configuration with $N = 15$ and $L_p = 3$, the number of multiplications for the conventional and the proposed algorithms are 4043 and 1550, respectively. The number of additions for them are 3522 and 1185, respectively. Compared to the CCM-RLS algorithm with the blind GVFF mechanism, the CCM-RLS algorithm with the proposed TAVFF mechanism reduces the computational complexity significantly. It is worth mentioning that the TAVFF mechanism alone requires 4 multiplications and 2 additions, whereas the blind GVFF algorithm alone requires $10M^2 + 16M + 7$ multiplications and $10M^2 + 6M - 1$ additions.

TABLE I
COMPUTATIONAL COMPLEXITY.

Algorithm	Number of operations per symbol	
	Multiplications	Additions
TAVFF	$6M^2 + L_p M + 10M + 5$	$5M^2 + L_p M + M$
Blind GVFF	$16M^2 + L_p M + 26M + 8$	$15M^2 + L_p M + 7M - 3$

V. ANALYSES OF THE PROPOSED ALGORITHM

In this section, we first theoretically show the convergence of the mean weight vector of the CCM-RLS receiver with the proposed TAVFF mechanism and derive the steady-state MSE expression of the proposed blind adaptive algorithm in the scenario of time-invariant channels. Then, we examine the tracking properties of the proposed algorithm in a time-varying environment.

A. Convergence of the Mean Weight Vector

In this part, we make some approximations and derive several expressions to show the convergence of the mean weight vector for the CCM-RLS receivers with the proposed TAVFF mechanism in the scenario of time-invariant channels.

Firstly, let us give two equations

$$\mathbf{s}_k(i) = \mathbf{Q}_k^{-1}(i)\mathbf{u}_k(i) \quad (29)$$

and

$$\gamma(i)\Gamma(i) = \beta(i)\mathbf{h}^H\mathbf{C}_k^H\mathbf{s}_k(i). \quad (30)$$

We will employ (29) and (30) in the following derivation. The proof is given in the appendix.

Let $\beta(i) = \frac{1}{\mathbf{h}^H\mathbf{C}_k^H\mathbf{f}(i)}$, where $\mathbf{f}(i) = \mathbf{Q}_k^{-1}(i)\mathbf{C}_k\mathbf{h}$, $\beta^{-1}(i) = \mathbf{h}^H\mathbf{C}_k^H\mathbf{f}(i)$. Here, we use \mathbf{h} in lieu of $\mathbf{h}(i)$. By multiplying $\mathbf{C}_k\mathbf{h}$ on both sides of (14), we have

$$\mathbf{f}(i) = \gamma^{-1}(i)\mathbf{f}(i-1) - \gamma^{-1}(i)\mathbf{s}_k(i)\mathbf{u}_k^H(i)\mathbf{f}(i-1), \quad (31)$$

and

$$\begin{aligned} \beta^{-1}(i) &= \gamma^{-1}(i)\mathbf{h}^H\mathbf{C}_k^H\mathbf{f}(i-1) - \gamma^{-1}(i)\mathbf{h}^H\mathbf{C}_k^H\mathbf{s}_k(i)\mathbf{u}_k^H(i)\mathbf{f}(i-1) \\ &= \gamma^{-1}(i)[\beta^{-1}(i-1) - \mathbf{h}^H\mathbf{C}_k^H\mathbf{s}_k(i)\mathbf{u}_k^H(i)\mathbf{f}(i-1)]. \end{aligned} \quad (32)$$

Thus, we can write

$$\beta(i) = \gamma(i)[\beta(i-1) + \beta(i-1)\Gamma(i)\mathbf{u}_k^H(i)\mathbf{f}(i-1)], \quad (33)$$

where

$$\Gamma(i) = \frac{\beta(i-1)\mathbf{h}^H \mathbf{C}_k^H \mathbf{s}_k(i)}{1 - \mathbf{h}^H \mathbf{C}_k^H \mathbf{s}_k(i) \mathbf{u}_k^H(i) \mathbf{f}(i-1) \beta(i-1)}. \quad (34)$$

By defining $\boldsymbol{\omega}(i) = \mathbf{h}^H \mathbf{C}_k^H \mathbf{Q}_k^{-1}(i) \mathbf{d}_k(i) \mathbf{C}_k \mathbf{h} - \nu \mathbf{C}_k \mathbf{h}$, we rewrite (12) as

$$\begin{aligned} \mathbf{w}_k(i) &= \beta(i) \mathbf{Q}_k^{-1}(i) (\beta^{-1}(i) \mathbf{d}_k(i) - \boldsymbol{\omega}(i)) \\ &= \gamma(i) \beta(i-1) (\gamma^{-1}(i) \mathbf{Q}_k^{-1}(i-1) (\beta^{-1}(i) \mathbf{d}_k(i) - \boldsymbol{\omega}(i)) \\ &\quad - \gamma^{-1}(i) \mathbf{s}_k(i) \mathbf{u}_k^H(i) \mathbf{Q}_k^{-1}(i-1) (\beta^{-1}(i) \mathbf{d}_k(i) - \boldsymbol{\omega}(i))) \\ &\quad + \gamma(i) \beta(i-1) \Gamma(i) \mathbf{u}_k^H(i) \mathbf{f}(i-1) \mathbf{Q}_k^{-1}(i) (\beta^{-1}(i) \mathbf{d}_k(i) - \boldsymbol{\omega}(i)). \end{aligned} \quad (35)$$

Let $\chi(i) = \beta(i-1) \mathbf{u}_k^H(i) \mathbf{f}(i-1)$, and using (29) we have

$$\begin{aligned} \mathbf{w}_k(i) &= \beta(i-1) \mathbf{Q}_k^{-1}(i-1) (\beta^{-1}(i) \mathbf{d}_k(i) - \boldsymbol{\omega}(i)) \\ &\quad - \mathbf{Q}_k^{-1}(i) \mathbf{u}_k(i) \mathbf{u}_k^H(i) \beta(i-1) \mathbf{Q}_k^{-1}(i-1) (\beta^{-1}(i) \mathbf{d}_k(i) - \boldsymbol{\omega}(i)) \\ &\quad + \gamma(i) \Gamma(i) \chi(i) \mathbf{Q}_k^{-1}(i) (\beta^{-1}(i) \mathbf{d}_k(i) - \boldsymbol{\omega}(i)). \end{aligned} \quad (36)$$

Based on [19], [20], [21], [25] and by adjusting the parameter ν to have the convexity of the CCM design [14], [15], we make the following assumptions

$$\begin{aligned} \lim_{i \rightarrow \infty} \mathbf{Q}_k^{-1}(i) &\approx \lim_{i \rightarrow \infty} E[\mathbf{Q}_k^{-1}(i)] \approx (1 - E[\gamma(\infty)]) \bar{\mathbf{Q}}_0^{-1} \\ &\approx (1 - E[\gamma(\infty)]) E^{-1}[|z_0(i)|^2] \mathbf{R}^{-1}, \end{aligned} \quad (37)$$

and

$$\lim_{i \rightarrow \infty} \mathbf{d}_k(i) \approx \lim_{i \rightarrow \infty} E[\mathbf{d}_k(i)] \approx \frac{1}{1 - E[\gamma(\infty)]} \bar{\mathbf{d}}_0. \quad (38)$$

The derivation of (37) and (38) is shown in the Appendix. Thus, when $i \rightarrow \infty$ we assume $\beta^{-1}(i) \mathbf{d}_k(i) - \boldsymbol{\omega}(i) \approx \beta^{-1}(i-1) \mathbf{d}_k(i-1) - \boldsymbol{\omega}(i-1)$. Subsequently, we rewrite (36) as

$$\begin{aligned} \mathbf{w}_k(i) &\approx \mathbf{w}_k(i-1) - \mathbf{Q}_k^{-1}(i) \mathbf{u}_k(i) \mathbf{u}_k^H(i) \mathbf{w}_k(i-1) \\ &\quad + \gamma(i) \Gamma(i) \chi(i) \mathbf{Q}_k^{-1}(i) (\beta^{-1}(i) \mathbf{d}_k(i) - \boldsymbol{\omega}(i)). \end{aligned} \quad (39)$$

By multiplying $\mathbf{Q}_k(i)$ and substituting $\mathbf{Q}_k(i) = \gamma(i) \mathbf{Q}_k(i-1) + \mathbf{u}_k(i) \mathbf{u}_k^H(i)$ we obtain

$$\begin{aligned} \mathbf{Q}_k(i) \mathbf{w}_k(i) &\approx \gamma(i) \mathbf{Q}_k(i-1) \mathbf{w}_k(i-1) + \mathbf{u}_k(i) \mathbf{u}_k^H(i) \mathbf{w}_k(i-1) - \mathbf{u}_k(i) \mathbf{u}_k^H(i) \mathbf{w}_k(i-1) \\ &\quad + \gamma(i) \mathbf{Q}_k(i) \Gamma(i) \chi(i) \mathbf{Q}_k^{-1}(i) (\beta^{-1}(i) \mathbf{d}_k(i) - \boldsymbol{\omega}(i)) \\ &= \gamma(i) \mathbf{Q}_k(i-1) \mathbf{w}_k(i-1) + \gamma(i) \Gamma(i) \chi(i) (\beta^{-1}(i) \mathbf{d}_k(i) - \boldsymbol{\omega}(i)). \end{aligned} \quad (40)$$

Let $\boldsymbol{\epsilon}(i) = \mathbf{w}_k(i) - \mathbf{w}_0$, and we have

$$\mathbf{Q}_k(i) \boldsymbol{\epsilon}(i) \approx \gamma(i) \mathbf{Q}_k(i-1) \boldsymbol{\epsilon}(i-1) + \mathbf{y}(i), \quad (41)$$

where

$$\begin{aligned}\mathbf{y}(i) &= \gamma(i)\Gamma(i)\chi(i)(\beta^{-1}(i)\mathbf{d}_k(i) - \boldsymbol{\omega}(i)) - \mathbf{u}_k(i)\mathbf{u}_k^H(i)\mathbf{w}_0 \\ &= \beta(i)(\beta^{-1}(i)\mathbf{d}_k(i) - \boldsymbol{\omega}(i))\mathbf{h}^H\mathbf{C}_k^H\mathbf{s}_k(i)\mathbf{u}_k^H(i)\beta(i-1)\mathbf{f}(i-1) - \mathbf{u}_k(i)\mathbf{u}_k^H(i)\mathbf{w}_0,\end{aligned}\quad (42)$$

where we have used (30). Using (37), when i becomes large, note that $\beta(i-1)\mathbf{f}(i-1) = \frac{\mathbf{Q}^{-1}(i-1)\mathbf{C}_k\mathbf{h}}{\mathbf{h}^H\mathbf{C}_k^H\mathbf{Q}^{-1}(i-1)\mathbf{C}_k\mathbf{h}} \approx \frac{\mathbf{R}^{-1}\mathbf{C}_k\mathbf{h}}{\mathbf{h}^H\mathbf{C}_k^H\mathbf{R}^{-1}\mathbf{C}_k\mathbf{h}}$ is the optimum minimum variance receiver in multipath channels [3]. Letting $\mathbf{v}_0 = \frac{\mathbf{R}^{-1}\mathbf{C}_k\mathbf{h}}{\mathbf{h}^H\mathbf{C}_k^H\mathbf{R}^{-1}\mathbf{C}_k\mathbf{h}}$, we obtain

$$\mathbf{Q}_k^{-1}(i)\mathbf{y}(i) = \beta(i)\mathbf{Q}_k^{-1}(i)(\beta^{-1}(i)\mathbf{d}_k(i) - \boldsymbol{\omega}(i))\mathbf{h}^H\mathbf{C}_k^H\mathbf{s}_k(i)\mathbf{u}_k^H(i)\mathbf{v}_0 - \mathbf{Q}_k^{-1}(i)\mathbf{u}_k(i)\mathbf{u}_k^H(i)\mathbf{w}_0. \quad (43)$$

Using (37) and (38) and recalling (7), we have

$$\lim_{i \rightarrow \infty} \beta(i)\mathbf{Q}_k^{-1}(i)(\beta^{-1}(i)\mathbf{d}_k(i) - \boldsymbol{\omega}(i)) \approx \mathbf{w}_0. \quad (44)$$

Thus, we obtain

$$\lim_{i \rightarrow \infty} \mathbf{Q}_k^{-1}(i)\mathbf{y}(i) \approx \mathbf{w}_0\mathbf{h}^H\mathbf{C}_k^H\mathbf{s}_k(i)\mathbf{u}_k^H(i)\mathbf{v}_0 - \mathbf{Q}_k^{-1}(i)\mathbf{u}_k(i)\mathbf{u}_k^H(i)\mathbf{w}_0. \quad (45)$$

By multiplying $\mathbf{Q}_k^{-1}(i)$ on both sides of (41) we have $\boldsymbol{\epsilon}(i) \approx \gamma(i)\mathbf{Q}_k^{-1}(i)\mathbf{Q}_k(i-1)\boldsymbol{\epsilon}(i-1) + \mathbf{Q}_k^{-1}(i)\mathbf{y}(i)$. When $i \rightarrow \infty$, it is given by

$$\boldsymbol{\epsilon}(i) \approx \gamma(i)\boldsymbol{\epsilon}(i-1) + \mathbf{w}_0\mathbf{h}^H\mathbf{C}_k^H\mathbf{s}_k(i)\mathbf{u}_k^H(i)\mathbf{v}_0 - \mathbf{Q}_k^{-1}(i)\mathbf{u}_k(i)\mathbf{u}_k^H(i)\mathbf{w}_0, \quad (46)$$

where $\mathbf{Q}_k^{-1}(i)\mathbf{Q}_k(i-1) \approx \mathbf{I}$.

By taking the expectation and due to the fact that, when i becomes large,

$$\begin{aligned}E[\mathbf{s}_k(i)\mathbf{u}_k^H(i)] &= E[\mathbf{Q}_k^{-1}(i)\mathbf{u}_k(i)\mathbf{u}_k^H(i)] \\ &\approx (1 - E[\gamma(i)])\bar{\mathbf{Q}}_0^{-1}E[\mathbf{u}_k(i)\mathbf{u}_k^H(i)] \\ &= (1 - E[\gamma(i)])\mathbf{I},\end{aligned}\quad (47)$$

we have

$$E[\boldsymbol{\epsilon}(i)] \approx E[\gamma(i)]E[\boldsymbol{\epsilon}(i-1)] + (1 - E[\gamma(i)])\mathbf{w}_0\mathbf{h}^H\mathbf{C}_k^H\mathbf{v}_0 - (1 - E[\gamma(i)])\mathbf{w}_0. \quad (48)$$

Using $\mathbf{h}^H\mathbf{C}_k^H\mathbf{v}_0 = 1$, finally we obtain

$$E[\boldsymbol{\epsilon}(i)] \approx E[\gamma(i)]E[\boldsymbol{\epsilon}(i-1)]. \quad (49)$$

Since $0 < E[\gamma(i)] < 1$, the expected weight error converges to zero.

B. Convergence of MSE

Then, we show the convergence of MSE for the proposed algorithm and give an analytical expression to predict the steady-state MSE.

When $i \rightarrow \infty$, we assume

$$\begin{aligned} E[\mathbf{u}_k(i)\mathbf{u}_k^H(i)] &= E[|z_0(i)|^2\mathbf{r}_k(i)\mathbf{r}_k^H(i)] \\ &\approx E[|z_0(i)|^2]E[\mathbf{r}_k(i)\mathbf{r}_k^H(i)] \\ &= E[|z_0(i)|^2]\mathbf{R}. \end{aligned} \quad (50)$$

Using (46) we have

$$\begin{aligned} \Theta(i) &= E[\boldsymbol{\epsilon}(i)\boldsymbol{\epsilon}^H(i)] \\ &\approx E[\gamma^2(i)]\Theta(i-1) + (1-E[\gamma(i)])^2\bar{\zeta}_1\mathbf{w}_0\mathbf{h}^H\mathbf{C}_k^H\mathbf{R}^{-1}\mathbf{C}_k\mathbf{h}\mathbf{w}_0^H - (1-E[\gamma(i)])^2\bar{\zeta}_2\mathbf{w}_0\mathbf{h}^H\mathbf{C}_k^H\mathbf{R}^{-1} \\ &\quad - (1-E[\gamma(i)])^2\bar{\zeta}_3\mathbf{R}^{-1}\mathbf{C}_k\mathbf{h}\mathbf{w}_0^H + (1-E[\gamma(i)])^2\bar{\zeta}_4\mathbf{R}^{-1}, \end{aligned} \quad (51)$$

where $\bar{\zeta}_1 = E[|\mathbf{v}_0^H\mathbf{r}(i)|^2] = \mathbf{v}_0^H\mathbf{R}\mathbf{v}_0$, $\bar{\zeta}_2 = E[\mathbf{w}_0^H\mathbf{r}(i)\mathbf{r}^H(i)\mathbf{v}_0] = \mathbf{w}_0^H\mathbf{R}\mathbf{v}_0$, $\bar{\zeta}_3 = E[\mathbf{v}_0^H\mathbf{r}(i)\mathbf{r}^H(i)\mathbf{w}_0] = \mathbf{v}_0^H\mathbf{R}\mathbf{w}_0$, and $\bar{\zeta}_4 = E[|\mathbf{w}_0^H\mathbf{r}(i)|^2] = \mathbf{w}_0^H\mathbf{R}\mathbf{w}_0$. Note that the steady-state MSE is given by

$$\begin{aligned} \lim_{i \rightarrow \infty} \xi_{mse}(i) &= \lim_{i \rightarrow \infty} E[|A_k b(i) - \mathbf{w}_k^H(i)\mathbf{r}(i)|^2] \\ &\approx \lim_{i \rightarrow \infty} (\Xi(i) + A_k^2 - A_k^2\mathbf{w}_0^H\mathbf{C}_k\mathbf{h} - A_k^2\mathbf{h}^H\mathbf{C}_k^H\mathbf{w}_0) \\ &= \lim_{i \rightarrow \infty} \Xi(i) + (1-2\nu)A_k^2, \end{aligned} \quad (52)$$

where $\mathbf{w}_0^H\mathbf{C}_k\mathbf{h} = \nu$ and

$$\begin{aligned} \Xi(i) &= E[(\boldsymbol{\epsilon}^H(i) + \mathbf{w}_0^H)\mathbf{r}(i)\mathbf{r}^H(i)(\boldsymbol{\epsilon}(i) + \mathbf{w}_0)] \\ &\approx \bar{\zeta}_4 + \text{tr}[\mathbf{R}\Theta(i)] + E[\boldsymbol{\epsilon}^H(i)]E[\mathbf{r}(i)\mathbf{r}^H(i)\mathbf{w}_0] + E[\mathbf{w}_0^H\mathbf{r}(i)\mathbf{r}^H(i)]E[\boldsymbol{\epsilon}(i)]. \end{aligned} \quad (53)$$

Since $\lim_{i \rightarrow \infty} E[\boldsymbol{\epsilon}(i)] = 0$, we have $\Xi(i) \approx \bar{\zeta}_4 + \Xi_{ex}(i)$, where $\Xi_{ex}(i) = \text{tr}[\mathbf{R}\Theta(i)]$ denotes the steady-state excess MSE. Multiplying (51) by \mathbf{R} we have

$$\begin{aligned} \text{tr}[\mathbf{R}\Theta(i)] &\approx E[\gamma^2(i)]\text{tr}[\mathbf{R}\Theta(i-1)] + (1-E[\gamma(i)])^2\bar{\zeta}_1\text{tr}[\mathbf{R}\mathbf{w}_0\mathbf{h}^H\mathbf{C}_k^H\mathbf{R}^{-1}\mathbf{C}_k\mathbf{h}\mathbf{w}_0^H] \\ &\quad - (1-E[\gamma(i)])^2\bar{\zeta}_2\text{tr}[\mathbf{R}\mathbf{w}_0\mathbf{h}^H\mathbf{C}_k^H\mathbf{R}^{-1}] - (1-E[\gamma(i)])^2\bar{\zeta}_3\text{tr}[\mathbf{C}_k\mathbf{h}\mathbf{w}_0^H] \\ &\quad + (1-E[\gamma(i)])^2\bar{\zeta}_4M \\ &= E[\gamma^2(i)]\text{tr}[\mathbf{R}\Theta(i-1)] + (1-E[\gamma(i)])^2\bar{\zeta}_1\text{tr}[\mathbf{R}\mathbf{w}_0\mathbf{h}^H\mathbf{C}_k^H\mathbf{R}^{-1}\mathbf{C}_k\mathbf{h}\mathbf{w}_0^H] \\ &\quad - (1-E[\gamma(i)])^2\bar{\zeta}_2\nu - (1-E[\gamma(i)])^2\bar{\zeta}_3\nu + (1-E[\gamma(i)])^2\bar{\zeta}_4M. \end{aligned} \quad (54)$$

Since $0 < E[\gamma^2(i)] < 1$, $\text{tr}[\mathbf{R}\Theta(i)]$ converges. Finally, we have

$$\Xi_{ex}(\infty) \approx \frac{(1-E[\gamma(\infty)])^2}{1-E[\gamma^2(\infty)]} \{ \bar{\zeta}_1\text{tr}[\mathbf{R}\mathbf{w}_0\mathbf{h}^H\mathbf{C}_k^H\mathbf{R}^{-1}\mathbf{C}_k\mathbf{h}\mathbf{w}_0^H] - \bar{\zeta}_2\nu - \bar{\zeta}_3\nu + \bar{\zeta}_4M \}, \quad (55)$$

where $E[\gamma(\infty)]$ and $E[\gamma^2(\infty)]$ are given in (27) and (28).

C. Tracking Analysis

In this part, we examine the tracking properties of the proposed TAVFF scheme in a nonstationary environment, for which the optimum solution takes on a time-varying form. In this scenario, the blind adaptive algorithm is given the task of tracking the minimum point of the error-performance surface, which is no longer fixed. In time-varying channels, the optimum filter coefficients are considered to vary according to the model $\mathbf{w}_0(i) = \mathbf{w}_0(i-1) + \mathbf{q}(i)$, where $\mathbf{q}(i)$ denotes a random perturbation [26]. We assume that $\mathbf{q}(i)$ is an independently generated sequence with zero mean and positive definite autocorrelation matrix $E[\mathbf{q}(i)\mathbf{q}^H(i)]$. This is typical in the context of tracking analyses of adaptive filters [27], [28], [29].

In this work, we consider the case that the channel varies slowly. For large i , there exists an interval $[N_i, i]$, for which the channel coefficients are approximately equivalent. Since the channel varies slowly, the variance of the element in $\mathbf{q}(i)$, namely, $\frac{\text{tr}[E[\mathbf{q}(i)\mathbf{q}^H(i)]]}{M}$ is a small value. From the above, we assume that when i becomes large we have

$$\beta(i)\mathbf{Q}_k^{-1}(i)(\beta^{-1}(i)\mathbf{d}_k(i) - \boldsymbol{\omega}(i)) \approx \mathbf{w}_0(i), \quad (56)$$

$$\beta(i-1)\mathbf{f}(i-1) \approx \mathbf{v}_0(i-1), \quad (57)$$

$$\mathbf{Q}_k^{-1}(i)\mathbf{Q}_k(i-1) \approx \mathbf{I}, \quad (58)$$

where $\mathbf{w}_0(i)$ and $\mathbf{v}_0(i-1)$ denote the optimum CCM receiver of time instant i and the optimum minimum variance receiver of time instant $i-1$, respectively, and the expression (40) still holds.

By redefining $\boldsymbol{\epsilon}(i) = \mathbf{w}(i) - \mathbf{w}_0(i)$ and recalling (40) we have

$$\mathbf{Q}_k(i)\boldsymbol{\epsilon}(i) \approx \gamma(i)\mathbf{Q}_k(i-1)\boldsymbol{\epsilon}(i-1) + \bar{\mathbf{y}}(i), \quad (59)$$

where

$$\begin{aligned} \bar{\mathbf{y}}(i) &= \gamma(i)\Gamma(i)\chi(i)(\beta^{-1}(i)\mathbf{d}_k(i) - \boldsymbol{\omega}(i)) - \gamma(i)\mathbf{Q}_k(i-1)\mathbf{q}(i) - \mathbf{u}_k(i)\mathbf{u}_k^H(i)\mathbf{w}_0(i) \\ &= \beta(i)(\beta^{-1}(i)\mathbf{d}_k(i) - \boldsymbol{\omega}(i))\mathbf{h}^H(i)\mathbf{C}_k^H\mathbf{s}_k(i)\mathbf{u}_k^H(i)\beta(i-1)\mathbf{f}(i-1) \\ &\quad - \gamma(i)\mathbf{Q}_k(i-1)\mathbf{q}(i) - \mathbf{u}_k(i)\mathbf{u}_k^H(i)\mathbf{w}_0(i). \end{aligned} \quad (60)$$

By multiplying $\mathbf{Q}_k^{-1}(i)$ on both sides of (59) we have

$$\boldsymbol{\epsilon}(i) \approx \gamma(i)\mathbf{Q}_k^{-1}(i)\mathbf{Q}_k(i-1)\boldsymbol{\epsilon}(i-1) + \mathbf{Q}_k^{-1}(i)\bar{\mathbf{y}}(i), \quad (61)$$

where

$$\begin{aligned} \mathbf{Q}_k^{-1}(i)\bar{\mathbf{y}}(i) &= \beta(i)\mathbf{Q}_k^{-1}(i)(\beta^{-1}(i)\mathbf{d}_k(i) - \boldsymbol{\omega}(i))\mathbf{h}^H(i)\mathbf{C}_k^H\mathbf{s}_k(i)\mathbf{u}_k^H(i)\mathbf{v}_0(i-1) \\ &\quad - \gamma(i)\mathbf{Q}_k^{-1}(i)\mathbf{Q}_k(i-1)\mathbf{q}(i) - \mathbf{Q}_k^{-1}(i)\mathbf{u}_k(i)\mathbf{u}_k^H(i)\mathbf{w}_0(i) \\ &\approx \mathbf{w}_0(i)\mathbf{h}^H(i)\mathbf{C}_k^H\mathbf{s}_k(i)\mathbf{u}_k^H(i)\mathbf{v}_0(i-1) - \gamma(i)\mathbf{q}(i) - \mathbf{Q}_k^{-1}(i)\mathbf{u}_k(i)\mathbf{u}_k^H(i)\mathbf{w}_0(i). \end{aligned} \quad (62)$$

Based on (61) and (62), we obtain

$$\begin{aligned}\boldsymbol{\epsilon}(i) &\approx \gamma(i)\boldsymbol{\epsilon}(i-1) + \mathbf{w}_0(i)\mathbf{h}^H(i)\mathbf{C}_k^H\mathbf{s}_k(i)\mathbf{u}_k^H(i)\mathbf{v}_0(i-1) - \gamma(i)\mathbf{q}(i) \\ &\quad - \mathbf{Q}_k^{-1}(i)\mathbf{u}_k(i)\mathbf{u}_k^H(i)\mathbf{w}_0(i).\end{aligned}\tag{63}$$

By taking the expectation of (63) and following the aforementioned approach, we can see that the expected weight error $E[\boldsymbol{\epsilon}(i)]$ converges to zero when the channel varies slowly.

Subsequently, we have

$$\begin{aligned}\boldsymbol{\Theta}(i) &= E[\boldsymbol{\epsilon}(i)\boldsymbol{\epsilon}^H(i)] \\ &\approx E[\gamma^2(i)]\boldsymbol{\Theta}(i-1) + (1-E[\gamma(i)])^2\bar{\zeta}_1(i)\mathbf{w}_0(i)\mathbf{h}^H(i)\mathbf{C}_k^H\mathbf{R}^{-1}(i)\mathbf{C}_k\mathbf{h}(i)\mathbf{w}_0^H(i) \\ &\quad - (1-E[\gamma(i)])^2\bar{\zeta}_2(i)\mathbf{w}_0(i)\mathbf{h}^H(i)\mathbf{C}_k^H\mathbf{R}^{-1}(i) - (1-E[\gamma(i)])^2\bar{\zeta}_3(i)\mathbf{R}^{-1}(i)\mathbf{C}_k\mathbf{h}(i)\mathbf{w}_0^H(i) \\ &\quad + (1-E[\gamma(i)])^2\bar{\zeta}_4(i)\mathbf{R}^{-1}(i) + E[\gamma^2(i)]E[\mathbf{q}(i)\mathbf{q}^H(i)],\end{aligned}\tag{64}$$

where $\bar{\zeta}_1(i) = E[|\mathbf{v}_0^H(i-1)\mathbf{r}(i)|^2] = \mathbf{v}_0^H(i-1)\mathbf{R}(i)\mathbf{v}_0(i-1)$, $\bar{\zeta}_2(i) = E[\mathbf{w}_0^H(i)\mathbf{r}(i)\mathbf{r}^H(i)\mathbf{v}_0(i-1)] = \mathbf{w}_0^H(i)\mathbf{R}(i)\mathbf{v}_0(i-1)$, $\bar{\zeta}_3(i) = E[\mathbf{v}_0^H(i-1)\mathbf{r}(i)\mathbf{r}^H(i)\mathbf{w}_0(i)] = \mathbf{v}_0^H(i-1)\mathbf{R}(i)\mathbf{w}_0(i)$, and $\bar{\zeta}_4(i) = E[|\mathbf{w}_0^H(i)\mathbf{r}(i)|^2] = \mathbf{w}_0^H(i)\mathbf{R}(i)\mathbf{w}_0(i)$.

When i becomes large, the steady-state MSE in the time-varying environment is given by

$$\begin{aligned}\xi_{mse}(i) &= E[|A_k b(i) - \mathbf{w}_k^H(i)\mathbf{r}(i)|^2] \\ &\approx \bar{\zeta}_4(i) + \Xi_{ex}(i) + A_k^2 - A_k^2\mathbf{w}_0^H(i)\mathbf{C}_k\mathbf{h}(i) - A_k^2\mathbf{h}^H(i)\mathbf{C}_k^H\mathbf{w}_0(i) \\ &= \bar{\zeta}_4(i) + \Xi_{ex}(i) + (1-2\nu)A_k^2,\end{aligned}\tag{65}$$

where $\mathbf{w}_0^H(i)\mathbf{C}_k\mathbf{h}(i) = \nu$ and $\Xi_{ex}(i) = \text{tr}[\mathbf{R}(i)\boldsymbol{\Theta}(i)]$ denotes the steady-state excess MSE in the time-varying scenario. By following the aforementioned approach we obtain

$$\begin{aligned}\Xi_{ex}(i) &\approx \frac{(1-E[\gamma(\infty)])^2}{1-E[\gamma^2(\infty)]}\{\bar{\zeta}_1(i)\text{tr}[\mathbf{R}(i)\mathbf{w}_0(i)\mathbf{h}^H(i)\mathbf{C}_k^H\mathbf{R}^{-1}(i)\mathbf{C}_k\mathbf{h}(i)\mathbf{w}_0^H(i)] - \bar{\zeta}_2(i)\nu - \bar{\zeta}_3(i)\nu + \bar{\zeta}_4(i)M \\ &\quad + \frac{E[\gamma^2(\infty)]}{(1-E[\gamma(\infty)])^2}\text{tr}[\mathbf{R}(i)E[\mathbf{q}(i)\mathbf{q}^H(i)]]\}.\end{aligned}\tag{66}$$

VI. SIMULATIONS

In this section, we evaluate the performance of the proposed TAVFF mechanism with the blind adaptive CCM-RLS receiver and compare it with the GVFF mechanism with the blind CCM-RLS receiver and the adaptive CCM-RLS and CMV-RLS receivers with the fixed forgetting factor mechanism. We adopt a simulation approach and conduct several experiments in order to verify the effectiveness of the TAVFF adaptive algorithm. The DS-CDMA system employs Gold sequences as the spreading codes, and the spreading gain is $N = 15$. The sequence of channel coefficients for each path is given by $h_f(i) = p_f\alpha_f(i)$ ($f = 0, 1, 2$). All channels are normalized so that

$$\sum_{f=0}^{L_p-1} p_f^2 = 1,\tag{67}$$

where $\alpha_f(i)$ is computed according to the Jakes' model [31]. For the blind CCM-RLS algorithms, the performance is not sensitive to the initial values, we set $\mathbf{d}_k(0) = \mathbf{0}$, $\mathbf{Q}_k^{-1}(0) = \mathbf{I}$ and $\mathbf{w}_k(0) = \mathbf{C}_k \hat{\mathbf{h}}(0)$, where $\hat{\mathbf{h}}(i)$ denotes the estimate of $\mathbf{h}(i)$ and we employ the blind adaptive channel estimation algorithm in [30]. The simulations are averaged over 10000 runs. We set the parameter $\nu = 1$ [14] and the power of the desired user $|A_1|^2 = 1$.

A. Effects of δ_1 and δ_2

We investigate the effects of δ_1 and δ_2 on the TAVFF mechanism, we show the received steady-state signal to interference plus noise ratio (SINR) versus δ_1 for $\delta_2 = 0.00015, 0.00008, 0.00003, 0.000015, 0.000006$ under different scenarios. We use $15dB$ for the input signal to noise ratio (SNR), and set $\gamma^- = 0.95$ and $\gamma^+ = 0.99998$ for the TAVFF mechanism to guarantee the stability. The results shown in Fig. 1 (a) and (b) are based on the channel with the normalized Doppler frequency $f_dT = 0.0001$. The channel has a power profile given by $p_0 = 0dB$, $p_1 = -6dB$ and $p_2 = -10dB$. In Fig. 1 (a), the system has 8 users including three users operating at a power level $3dB$ above and one user operating at a power level $6dB$ above the desired user's power level. In Fig. 1 (b), the system has 5 users including one with a power level $3dB$ above the desired user's power level. It is observed that, firstly, the optimum choice of the pair (δ_1, δ_2) is not unique, for each value of δ_2 we can find a relevant δ_1 to have the best performance. Secondly, when we increase the value of δ_2 , δ_1 should be reduced for an optimum pair. Thirdly, with the increasing of δ_2 the performance becomes less sensitive to δ_1 . Moreover, for a system with a low load, the performance becomes insensitive to δ_1 before it decreases dramatically. From the results, we can obtain that $\delta_1 = 0.9896$ and $\delta_2 = 0.00008$ are one of the best choices for the scenario in Fig. 1 (a) and $\delta_1 = 0.9822$ and $\delta_2 = 0.00015$ are one of the best choices for both scenarios.

The results in Fig. 2 (a) and (b) show the steady-state SINR versus δ_1 for different values of δ_2 based on the channel with $f_dT = 0.00005$. The channel has a power profile given by $p_0 = 0dB$, $p_1 = -6dB$ and $p_2 = -10dB$. In Fig. 2 (a), the system includes 8 users with the same power level. In Fig. 2 (b), the system has 5 users, power of which are equivalent. We can see that the previous findings on effects of δ_1 and δ_2 still hold for the experiments. In this case, we found that $\delta_1 = 0.9970$ and $\delta_2 = 0.000015$ are one of the best choices for both scenarios. In Fig. 3, we show the SINR performance versus the number of received symbols in terms of the simulation environment of Fig. 1 (a), where three pairs $(0.9970, 0.000015)$, $(0.9822, 0.00015)$ and $(0.9896, 0.00008)$ are employed for δ_1 and δ_2 . From the results in Fig. 3, we can see that the three choices provide almost the same convergence performance, which shows that it is possible for us to find a pair (δ_1, δ_2) that works well for different scenarios. In the following experiments, for a given scenario we first choose the optimum parameters, and then fix them through the simulations. In practice, these optimized values should be obtained by experimentation for a given range of values or a specific operating point, and stored at the receiver.

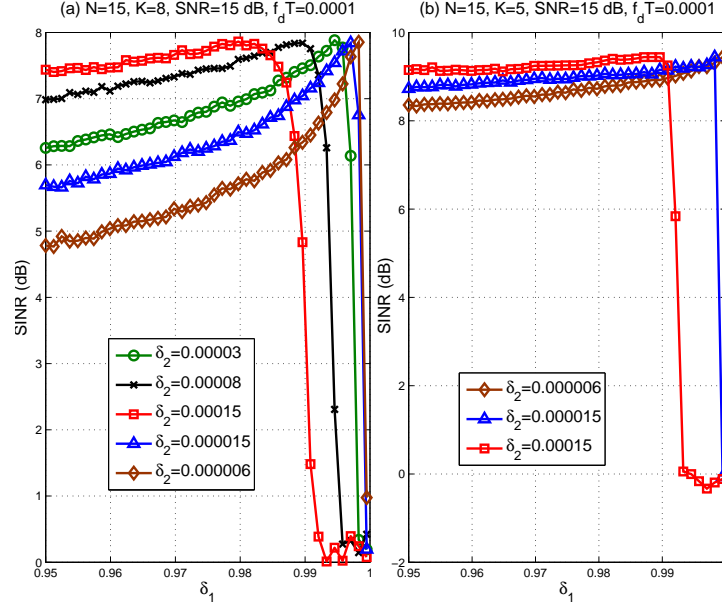


Fig. 1. Steady-state SINR versus δ_1 for different values of δ_2 , (a) $K = 8$, with three 3dB and one 6dB high power level interferers, (b) $K = 5$, with one 3dB high power level interferer. $\text{SNR} = 15 \text{ dB}$, $f_d T = 1 \times 10^{-4}$.

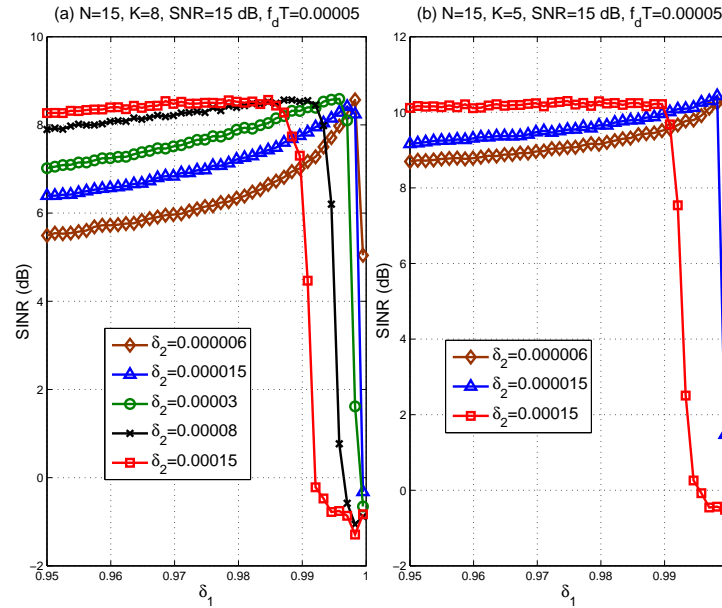


Fig. 2. Steady-state SINR versus δ_1 for different values of δ_2 , (a) $K = 8$, with equal power level interferers, (b) $K = 5$, with equal power level interferers. $\text{SNR} = 15 \text{ dB}$, $f_d T = 5 \times 10^{-5}$.

B. SINR Convergence Performance

We choose the received SINR as the performance index to evaluate the convergence performance in nonstationary scenarios. In the following experiments, we assess the SINR performance of the analyzed schemes, namely, the

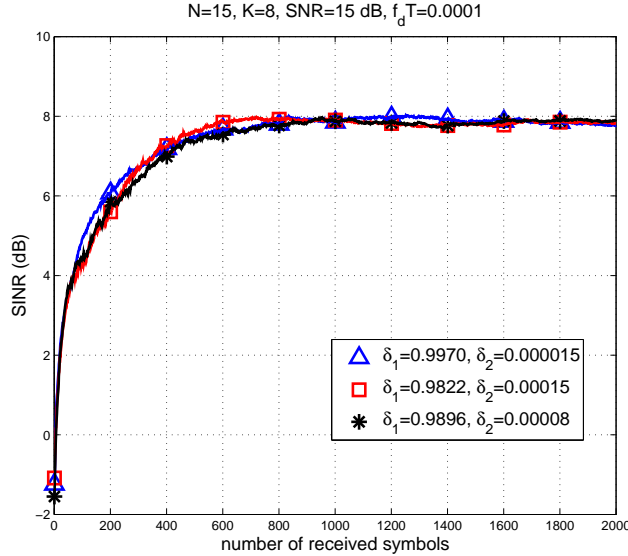


Fig. 3. SINR performance versus the number of received symbols for different values of δ_1 and δ_2 . $K = 8$, with three 3dB and one 6dB high power level interferers. SNR= 15dB, $f_d T = 1 \times 10^{-4}$.

proposed TAVFF, the multipath blind GVFF and the fixed forgetting factor mechanisms. The first experiment shown in Fig. 4 illustrates that the performance in terms of SINR of the analyzed algorithms in a nonstationary scenario with high power interferers. The system starts with five users including one high-power level interferer with 3dB above the desired one and after 1000 symbols, three new interferers including two users operating at a power level 3dB above and one user operating at a power level 6dB above the desired user's power level enter the system, where $f_d T = 1 \times 10^{-4}$. The channel has a power profile given by $p_0 = 0dB$, $p_1 = -6dB$ and $p_2 = -10dB$. From Fig. 4, we can see that the proposed TAVFF mechanism with the blind adaptive CCM-RLS receiver achieves the best performance, followed by the GVFF mechanism with the blind adaptive CCM-RLS receiver, the blind adaptive CCM-RLS and CMV-RLS receivers with the fixed forgetting factor mechanism. In this simulation, we have tuned the parameters of the mechanisms, as shown in Table II, where $\mathbf{1}$ denotes an all-one vector. We remark that the parameters of the blind GVFF and fixed forgetting factor mechanisms are tuned to optimize the performance.

TABLE II
OPTIMIZED PARAMETERS FOR CASE 1

Fixed Schemes	$\gamma = 0.998$
Blind GVFF	$\gamma(0) = 0.999, \mu = 0.00025, \frac{\partial \mathbf{Q}_k^{-1}(0)}{\partial \gamma} = \mathbf{I},$ $\mathbf{Y}_k(0) = 0.01 \times \mathbf{1}, \frac{\partial \mathbf{d}_k(0)}{\partial \gamma} = \mathbf{0}, \mathbf{s}_k(0) = \mathbf{0}$ $\gamma^- = 0.98, \gamma^+ = 0.99998$
TAVFF	$\phi(0) = 0, \delta_1 = 0.9822, \delta_2 = 0.00015$ $\gamma^- = 0.95, \gamma^+ = 0.99998$

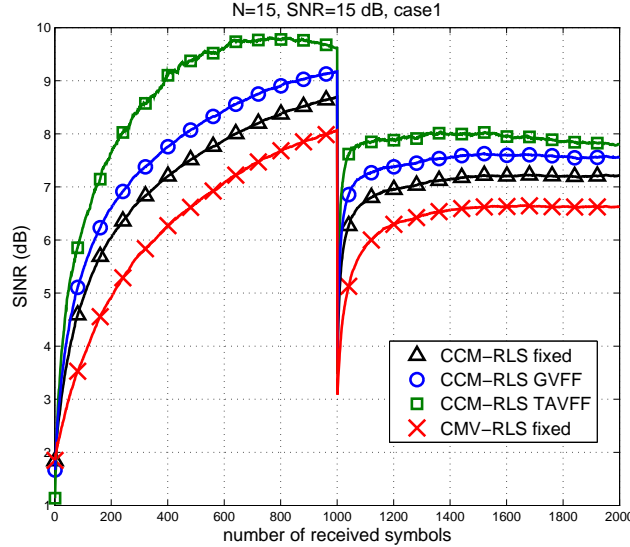


Fig. 4. SINR performance in nonstationary environment of multipath time varying channels. Case 1: with high power interferers. SNR= 15dB. $f_dT = 0.0001$.

The second experiment shown in Fig. 5 shows the SINR performance of the desired user versus the number of received symbols in a nonstationary scenario with equal power interferers for the proposed TAVFF scheme, the blind GVFF scheme and the conventional fixed forgetting factor schemes. In the simulation, the system starts with five users operating at equal power levels. At 1000 symbols, three interferers having the same power level as the first five users' enter the system. The normalized Doppler frequency is $f_dT = 5 \times 10^{-5}$. The channel has a power profile given by $p_0 = 0dB$, $p_1 = -6dB$ and $p_2 = -10dB$. We can see that the overall performance increases compared to the first experiment in Fig. 4 due to the lower power interferers and the CCM-RLS algorithm with the TAVFF scheme converges much faster than the GVFF scheme and fixed forgetting factor algorithms in multipath fading channels. For this case, we tuned the parameters of the mechanisms, as shown in Table III.

TABLE III
OPTIMIZED PARAMETERS FOR CASE 2

Fixed Schemes	$\gamma = 0.9992$
Blind GVFF	$\gamma(0) = 0.999, \mu = 0.0001, \frac{\partial \mathbf{Q}_k^{-1}(0)}{\partial \gamma} = \mathbf{I},$ $\mathbf{Y}_k(0) = 0.01 \times \mathbf{1}, \frac{\partial \mathbf{d}_k(0)}{\partial \gamma} = \mathbf{0}, \mathbf{s}_k(0) = \mathbf{0}$ $\gamma^- = 0.98, \gamma^+ = 0.99998$
TAVFF	$\phi(0) = 0, \delta_1 = 0.9970, \delta_2 = 0.000015$ $\gamma^- = 0.95, \gamma^+ = 0.99998$

The third experiment shown in Fig. 6 illustrates the variation of the forgetting factor values versus the number of received systems. The curves “Case 1” and “Case 2” correspond to the proposed TAVFF mechanism in the first

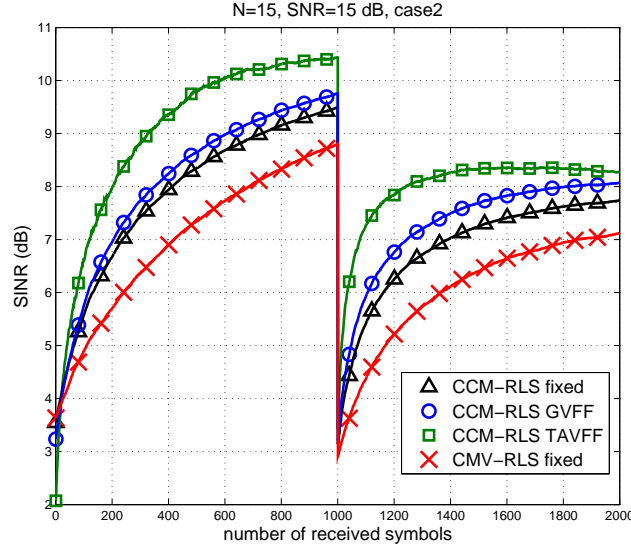


Fig. 5. SINR performance in nonstationary environment of multipath time varying channels. Case 2: with equal power interferers. SNR=15dB. $f_dT = 0.00005$.

and second experiments, respectively. We can see that the forgetting factor value becomes small at the first several iterations due to the large prediction error and it increases gradually until the system converges. At 1000 symbols, when the new interferers enter the system, the forgetting factor will be recomputed.

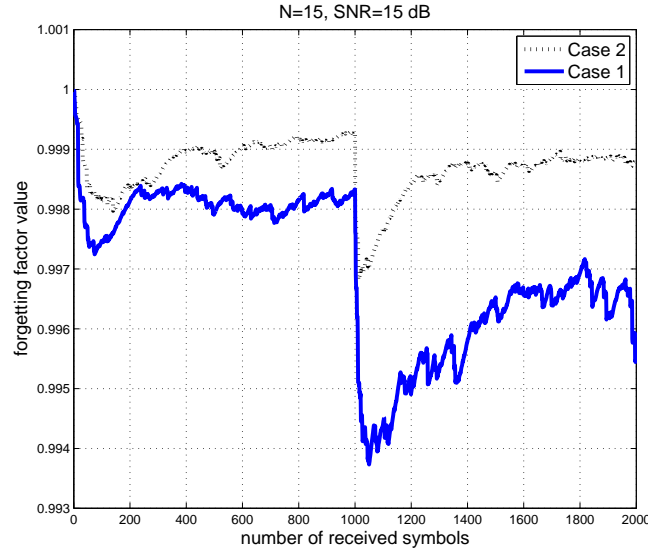


Fig. 6. Forgetting factor variation of the proposed TAVFF scheme in nonstationary scenarios. SNR= 15dB.

Next, we study the finite-word length effects on the variable forgetting factor $\gamma(i)$ for the proposed TAVFF mechanism. We employ B bits to represent the true value of $\gamma(i)$, which varies in the range from γ^- to γ^+ , where $\gamma^- = 0.95$ and $\gamma^+ = 0.99998$. We divide the range $[\gamma^-, \gamma^+]$ equally into 2^B intervals. When the true value drops

into a particular interval, we will use the left end-point of the relevant interval to replace it. Fig. 7 and 8 show the SINR convergence performance in nonstationary environments for finite-word length effects in terms of “Case 1” and “Case 2”, respectively. We use $B = 12$ and 8 bits for the simulation. From the results, we can see that using 12 bits to represent the variable forgetting factor does not degrade the performance. However, it degrades slightly when we reduce the number of bits to 8 for the variable forgetting factor. It shows the ability of the TAVFF mechanism to deal with finite-word length effects.

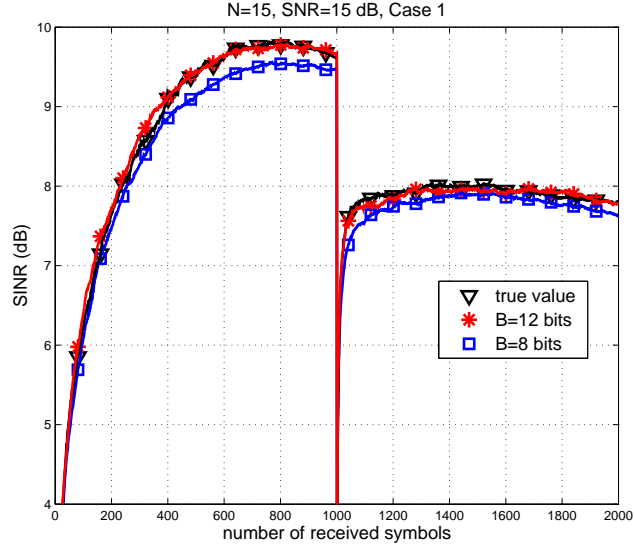


Fig. 7. SINR performance in a nonstationary environment for the finite-word length effects. Case 1: with high power interferers. SNR= 15dB. $f_dT = 0.0001$.

Finally, we examine the SINR performance of the TAVFF mechanism in a static environment. We compare the TAVFF mechanism with the blind GVFF and the fixed forgetting factor mechanisms. Fig. 9 illustrates the SINR performance versus the number of received symbols for a static environment, where the time-invariant channel parameters are given by $h_0 = 0dB$, $h_1 = -3dB$ and $h_2 = -6dB$. The system includes 5 users which have equal power level, SNR= 15dB. Fig. 9 shows that the proposed TAVFF mechanism still works well in a static environment, and it outperforms the other conventional schemes. In this simulation, we tuned the parameters of the mechanisms, as shown in Table IV.

C. BER Performance

In Fig. 10, we show the bit error rate (BER) performance of the following algorithms as the fading rate of the channel varies: the CCM-RLS receiver with the TAVFF mechanism, the CCM-RLS receiver with the GVFF mechanism, the CCM-RLS receiver with the fixed forgetting factor mechanism and the CMV-RLS receiver with the fixed forgetting factor mechanism. Monte-carlo simulations are conducted, for each simulation we use data packets

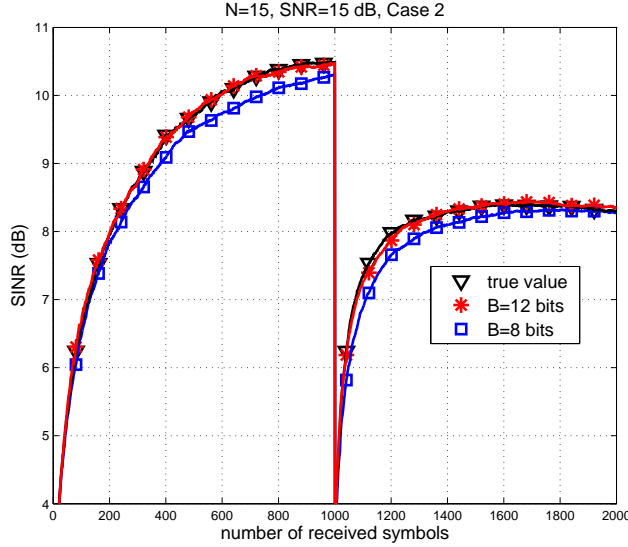


Fig. 8. SINR performance in a nonstationary environment for the finite-word length effects. Case 2: with equal power interferers. SNR = 15dB. $f_d T = 0.00005$.

TABLE IV
OPTIMIZED PARAMETERS FOR INVARIANT CHANNELS

Fixed Schemes	$\gamma = 0.999$
Blind GVFF	$\gamma(0) = 0.999$, $\mu = 0.005$, $\frac{\partial \mathbf{Q}_k^{-1}(0)}{\partial \gamma} = \mathbf{I}$, $\mathbf{Y}_k(0) = 0.01 \times \mathbf{1}$, $\frac{\partial \mathbf{d}_k(0)}{\partial \gamma} = \mathbf{0}$, $\mathbf{s}_k(0) = \mathbf{0}$ $\gamma^- = 0.998$, $\gamma^+ = 0.99998$
TAVFF	$\phi(0) = 0$, $\delta_1 = 0.98$, $\delta_2 = 0.00025$ $\gamma^- = 0.95$, $\gamma^+ = 0.99998$

with 1500 symbols for the blind adaptive algorithms. The system has five users operating at the same power level, and the SNR is 15dB. The channel has a power profile given by $p_0 = 0dB$, $p_1 = -6dB$ and $p_2 = -10dB$. We used $\delta_1 = 0.9822$, $\delta_2 = 0.00015$, $\gamma^- = 0.95$ and $\gamma^+ = 0.99998$ for the TAVFF mechanism. For the GVFF mechanism, we used $\gamma^- = 0.98$ and $\gamma^+ = 0.99998$, and tuned $\mu = 0.0001, 0.00016, 0.00026, 0.00045, 0.00045$ for $f_d T = 5 \times 10^{-5}, 5 \times 10^{-4}, 5 \times 10^{-3}, 5 \times 10^{-2}, 0.5$, respectively. First, we can see that, as the fading rate increases, the performance gets worse, and our proposed TAVFF scheme outperforms the existing schemes. Moreover, we observe that the CCM-RLS algorithm is better than the CMV-RLS algorithm. Second, Fig. 10 shows the ability of the CCM-RLS receiver with the TAVFF mechanism to deal with channel uncertainties. Note that the values of the forgetting factors for the algorithms which employ fixed forgetting factors are optimized. In this experiment, we tuned suitable forgetting factors for each “ $f_d T$ ”.

The results in Fig. 11 (a) and (b) show the BER performance of the desired user versus the SNR and the number of

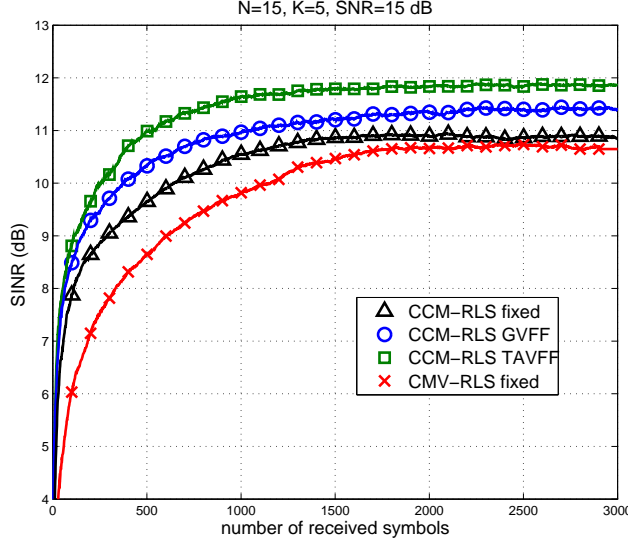


Fig. 9. SINR performance in a static environment. SNR= 15dB, K = 5.

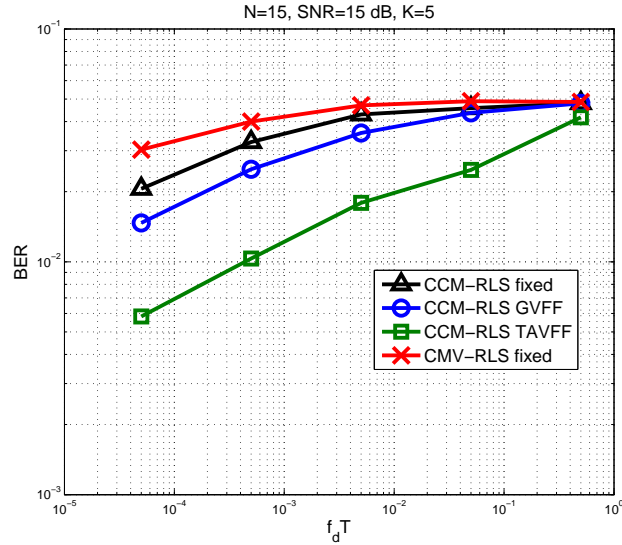


Fig. 10. BER versus f_dT (cycles/symbol) in multipath time varying channels. SNR= 15dB, K= 5.

users K for a static environment, where the time-invariant channel parameters are given by $h_0 = 0dB$, $h_1 = -3dB$ and $h_2 = -6dB$. We assume that the users operate with the same power level. For the TAVFF mechanism, we tuned $\gamma^- = 0.95$, $\gamma^+ = 0.99998$, $\delta_1 = 0.98$ and $\delta_2 = 0.00015$. For the GVFF mechanism, we tuned $\gamma^- = 0.998$, $\gamma^+ = 0.99998$ and $\mu = 0.001$. The results in Fig. 11 (a) and (b) indicate that the best performance is achieved with the proposed TAVFF mechanism, followed by the existing forgetting factor schemes. In particular, the CCM-RLS receiver with the TAVFF mechanism can save up to 3dB and support up to two more users in comparison with the CCM-RLS receiver with the blind GVFF mechanism at the BER level of 10^{-2} .

Fig. 12 (a) and (b) illustrate the BER performance of the desired user versus the SNR and the number of users

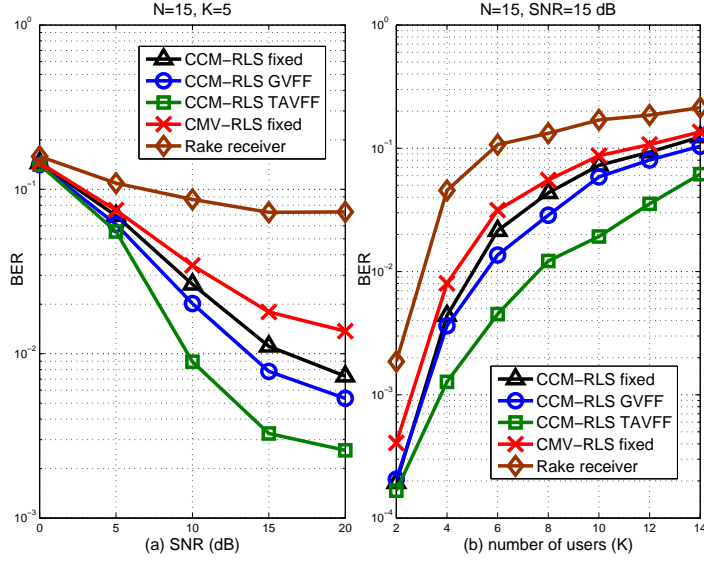


Fig. 11. BER performance versus (a) SNR and (b) the number of users (K) in a static environment.

K , where we set $f_d T = 5 \times 10^{-5}$. We assume that the users operate with the same power level. The channel has a power profile given by $p_0 = 0\text{dB}$, $p_1 = -6\text{dB}$ and $p_2 = -10\text{dB}$. For the TAVFF mechanism, we tuned $\gamma^- = 0.95$, $\gamma^+ = 0.99998$, $\delta_1 = 0.9822$ and $\delta_2 = 0.00015$. For the GVFF mechanism, we tuned $\gamma^- = 0.98$, $\gamma^+ = 0.99998$ and $\mu = 0.0001$. We can see that the best performance is achieved by the CCM-RLS receiver with the TAVFF mechanism, followed by the CCM-RLS receiver with the GVFF mechanism, the CCM-RLS receiver with the fixed forgetting factor mechanism, the CMV-RLS receiver with the fixed forgetting factor mechanism and the conventional Rake receiver. In particular, the CCM-RLS receiver with the TAVFF mechanism can save up to 5dB and support up to two more users in comparison with the CCM-RLS receiver with the fixed forgetting factor mechanism at the BER level of 10^{-2} .

D. MSE Performance: Analytical Results

In this part, we consider the convergence and tracking analyses of the proposed TAVFF mechanism with the CCM-RLS receiver. The steady-state MSE between the desired and the estimated symbol obtained through simulation is compared with the steady-state MSE computed via the expressions derived in Section V. Firstly, we verify that the analytical results (27), (28), (52) and (55) to predict the steady-state MSE in the case of invariant channels. Note that the work in [32] used a scaled version of the Wiener filter to approximate the optimum CCM solution w_0 . In this work, we employ the steady-state filter weights of the CCM-RLS algorithm as w_0 . The adaptive CCM algorithm has been verified to converge to a very close MSE value to that of the Wiener filter [15], [16], [32]. In this simulation of convergence analysis, we assume that five users having the same power level operate in the system. The time-invariant multipath scenario with AWGN is considered. The time-invariant channel parameters

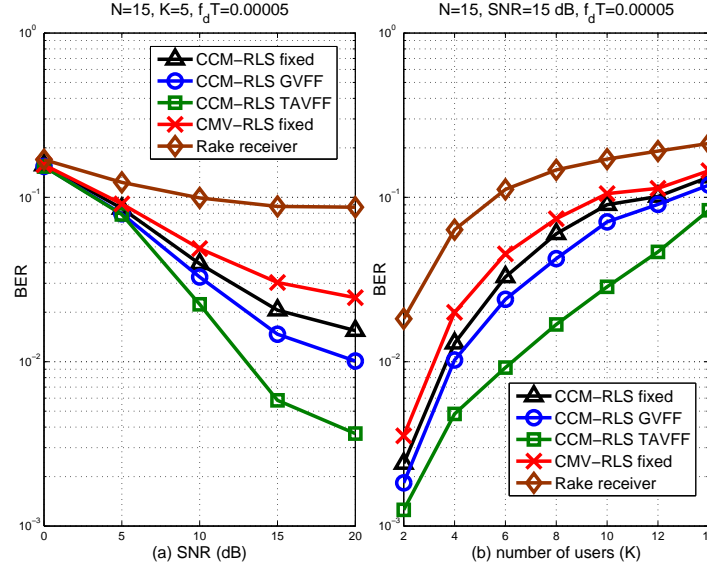


Fig. 12. BER performance versus (a) SNR and (b) the number of users (K) in multipath time varying channels, $f_d T = 5 \times 10^{-5}$.

are given by $h_0 = 0\text{dB}$, $h_1 = -6\text{dB}$ and $h_2 = -10\text{dB}$. By comparing the curves in Fig. 13 (a), it can be seen that as the number of received symbols increases and the simulated MSE converges to the analytical result, showing the usefulness of our analysis and assumptions, where $\delta_1 = 0.95$ and $\delta_2 = 0.00015$. Fig. 13 (b) shows the MSE performance versus the desired user's SNR, and a comparison between the steady-state analysis and simulation results. The simulation and analysis results agree well with each other.

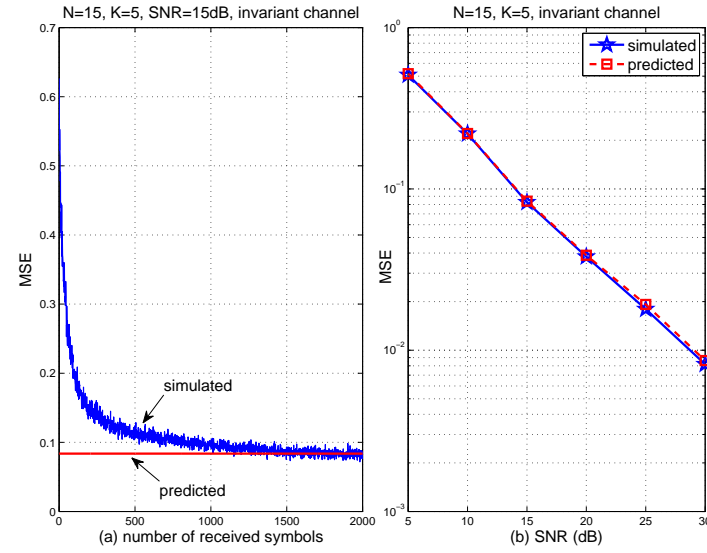


Fig. 13. Analytical MSE versus simulated performance for convergence analysis of the proposed TAVFF scheme in invariant channels. (a) the number of users is 5, SNR= 15dB. (b) the number of users is 5.

Secondly, we discuss the tracking analysis of the proposed TAVFF mechanism with the CCM-RLS receiver in a

fading channel. Here, we verify that the analytical results (27), (28), (65) and (66) are able to provide an accurate prediction of the steady-state MSE in a fading channel. In order to obtain the value of $E[\mathbf{q}(i)\mathbf{q}^H(i)]$, we run 10000 independent experiments, and for each experiment, $\mathbf{q}(i)$ is computed by $\mathbf{q}(i) = \mathbf{w}_0(i) - \mathbf{w}_0(i-1)$, where i is a large number to guarantee that the receiver works at the steady-state. The quantity of $E[\mathbf{q}(i)\mathbf{q}^H(i)]$ is estimated by using the average over the 10000 independent experiments, namely, $(\sum_{i=1}^{N_e} \mathbf{q}(i)\mathbf{q}^H(i))/N_e$, where $N_e = 10000$. In this simulation, we assume that five users operate with the same power level in the system. A time-varying channel with the normalized Doppler frequency $f_d T = 1 \times 10^{-5}$ is considered. The channel has a power profile given by $p_0 = 0dB$, $p_1 = -6dB$ and $p_2 = -10dB$. Fig. 14 (a) indicates that as the number of received symbols increases, the simulated MSE converges to the analytical result, showing the usefulness of our tracking analysis, where $\delta_1 = 0.98$ and $\delta_2 = 0.000015$. Fig. 14 (b) shows the effect that the desired user's SNR has on the MSE. We also can see that the simulation and analysis results agree well with each other.

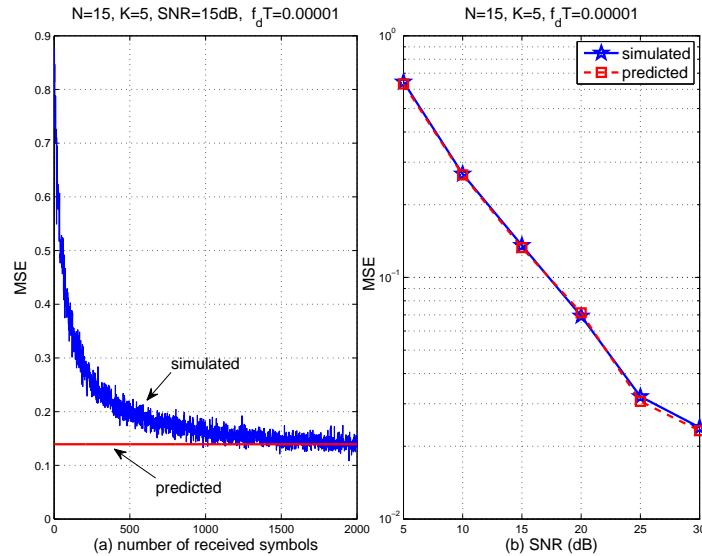


Fig. 14. Analytical MSE versus simulated performance for tracking analysis of the proposed TAVFF scheme. (a) the number of users is 5, SNR=15dB. (b) the number of users is 5. $f_d T = 1 \times 10^{-5}$.

VII. CONCLUSION

In this paper, we proposed a low-complexity variable forgetting factor mechanism for estimating the parameters of linear CDMA receivers that operate with RLS algorithms, and we also extended the conventional GVFF scheme to the blind CCM-RLS receiver in multipath fading channels. We compared the computational complexity of the new algorithm with the existent methods and further investigated the convergence and tracking analyses of the proposed TAVFF scheme. We also derived expressions to predict the steady-state MSE of the adaptive CCM-RLS algorithm with the TAVFF mechanism. The simulation results verify the analytical results and show that the proposed scheme

significantly outperforms existing algorithms and supports systems with higher loads. We remark that our proposed algorithm also can be extended to take into account other types of applications.

APPENDIX

A. The updated equations of $\mathbf{Y}_k(i)$, $\frac{\partial \mathbf{Q}_k^{-1}(i)}{\partial \gamma}$, $\frac{\partial \mathbf{d}_k(i)}{\partial \gamma}$ and $\frac{\partial \mathbf{s}_k(i)}{\partial \gamma}$ for the blind GVFF mechanism in multipath channels.

$$\begin{aligned} \mathbf{Y}_k &= \frac{\partial \mathbf{Q}_k^{-1}(i)}{\partial \gamma} \left(\mathbf{d}_k(i) - (\mathbf{h}^H \mathbf{C}_k^H \mathbf{Q}_k^{-1}(i) \mathbf{d}_k(i) \mathbf{C}_k \mathbf{h} - \nu \mathbf{C}_k \mathbf{h}) (\mathbf{h}^H \mathbf{C}_k^H \mathbf{Q}_k^{-1}(i) \mathbf{C}_k \mathbf{h})^{-1} \right) \\ &\quad + \mathbf{Q}_k^{-1}(i) \left(\frac{\partial \mathbf{d}_k(i)}{\partial \gamma} - (((\mathbf{h}^H \mathbf{C}_k^H \frac{\partial \mathbf{Q}_k^{-1}(i)}{\partial \gamma} \mathbf{d}_k(i) \mathbf{C}_k \mathbf{h} + \mathbf{h}^H \mathbf{C}_k^H \mathbf{Q}_k^{-1}(i) \frac{\partial \mathbf{d}_k(i)}{\partial \gamma} \mathbf{C}_k \mathbf{h}) \right. \right. \\ &\quad \times (\mathbf{h}^H \mathbf{C}_k^H \mathbf{Q}_k^{-1}(i) \mathbf{C}_k \mathbf{h}) - (\mathbf{h}^H \mathbf{C}_k^H \frac{\partial \mathbf{Q}_k^{-1}(i)}{\partial \gamma} \mathbf{C}_k \mathbf{h}) \\ &\quad \left. \left. \times (\mathbf{h}^H \mathbf{C}_k^H \mathbf{Q}_k^{-1}(i) \mathbf{d}_k(i) \mathbf{C}_k \mathbf{h} - \nu \mathbf{C}_k \mathbf{h})) \right) (\mathbf{h}^H \mathbf{C}_k^H \mathbf{Q}_k^{-1}(i) \mathbf{C}_k \mathbf{h})^{-2} \right), \end{aligned} \quad (68)$$

$$\begin{aligned} \frac{\partial \mathbf{Q}_k^{-1}(i)}{\partial \gamma} &= -\gamma^{-2} \mathbf{Q}_k^{-1}(i-1) + \gamma^{-1} \frac{\partial \mathbf{Q}_k^{-1}(i-1)}{\partial \gamma} + \gamma^{-2} \mathbf{s}_k(i) \mathbf{u}_k^H(i) \mathbf{Q}_k^{-1}(i-1) - \gamma^{-1} \frac{\partial \mathbf{s}_k(i)}{\partial \gamma} \mathbf{u}_k^H(i) \\ &\quad \times \mathbf{Q}_k^{-1}(i-1) - \gamma^{-1} \mathbf{s}_k(i) \mathbf{r}^H(i) (\mathbf{r}^H(i) \mathbf{Y}_k(i)) \mathbf{Q}_k^{-1}(i-1) - \gamma^{-1} \mathbf{s}_k(i) \mathbf{u}_k^H(i) \frac{\partial \mathbf{Q}_k^{-1}(i-1)}{\partial \gamma}, \end{aligned} \quad (69)$$

$$\frac{\partial \mathbf{d}_k(i)}{\partial \gamma} = \mathbf{d}_k(i-1) + \gamma \frac{\partial \mathbf{d}_k(i-1)}{\partial \gamma} - z_k^*(i) \mathbf{r}(i) + (1-\gamma) \mathbf{r}^H(i) \mathbf{Y}_k(i) \mathbf{r}(i), \quad (70)$$

and

$$\begin{aligned} \frac{\partial \mathbf{s}_k(i)}{\partial \gamma} &= \left\{ \left(\frac{\partial \mathbf{Q}_k^{-1}(i-1)}{\partial \gamma} \mathbf{u}_k(i) + \mathbf{Q}_k^{-1}(i-1) (\mathbf{Y}_k^H(i) \mathbf{r}(i)) \mathbf{r}(i) \right) \left(\gamma + \mathbf{u}_k^H(i) \mathbf{Q}_k^{-1}(i-1) \mathbf{u}_k(i) \right) \right. \\ &\quad - \mathbf{Q}_k^{-1}(i-1) \mathbf{u}_k(i) \left(1 + \mathbf{r}^H(i) (\mathbf{r}^H(i) \mathbf{Y}_k(i)) \mathbf{Q}_k^{-1}(i-1) \mathbf{u}_k(i) \right. \\ &\quad \left. \left. + \mathbf{u}_k^H(i) \frac{\partial \mathbf{Q}_k^{-1}(i-1)}{\partial \gamma} \mathbf{u}_k(i) + \mathbf{u}_k^H(i) \mathbf{Q}_k^{-1}(i-1) (\mathbf{Y}_k^H(i) \mathbf{r}(i)) \mathbf{r}(i) \right) \right\} \\ &\quad \times (\gamma + \mathbf{u}_k^H(i) \mathbf{Q}_k^{-1}(i-1) \mathbf{u}_k(i))^{-2}. \end{aligned} \quad (71)$$

B. Proof of (23)

Using (18) we write

$$\begin{aligned} E[\phi(i-1)(|\mathbf{w}_k^H(i)\mathbf{r}(i)|^2 - 1)^2] &= E[\phi(i-1)]E[(|\mathbf{w}_k^H(i)\mathbf{r}(i)|^2 - 1)^2] \\ &\quad + E[(\phi(i-1) - E[\phi(i-1)])(|\mathbf{w}_k^H(i)\mathbf{r}(i)|^2 - 1)^2]. \end{aligned} \quad (72)$$

Note that δ_2 is sufficiently small, and $\phi(i)$ is a small value. Based on (18), we claim that $\phi(i)$ varies slowly around its mean value. The second term on the right side of (72) is very small compared to the first term. Thus, we neglect the second term and obtain (23).

C. Proof of (29)

By multiplying $\mathbf{u}_k(i)$ on both sides of (14) we have

$$\mathbf{Q}_k^{-1}(i)\mathbf{u}_k(i) = \gamma^{-1}(i)\mathbf{Q}_k^{-1}(i-1)\mathbf{u}_k(i) - \gamma^{-1}(i)\mathbf{s}_k(i)\mathbf{u}_k^H(i)\mathbf{Q}_k^{-1}(i-1)\mathbf{u}_k(i). \quad (73)$$

Rewrite (13) as

$$\mathbf{s}_k(i) = \gamma^{-1}(i)\mathbf{Q}_k^{-1}(i-1)\mathbf{u}_k(i) - \gamma^{-1}(i)\mathbf{s}_k(i)\mathbf{u}_k^H(i)\mathbf{Q}_k^{-1}(i-1)\mathbf{u}_k(i). \quad (74)$$

Based on (73) and (74) we have (29).

D. Proof of (30)

By multiplying $\mathbf{h}^H\mathbf{C}_k^H\mathbf{s}_k(i)$ on both sides of (33) we have

$$\beta(i)\mathbf{h}^H\mathbf{C}_k^H\mathbf{s}_k(i) = \gamma(i)(\beta(i-1)\mathbf{h}^H\mathbf{C}_k^H\mathbf{s}_k(i) + \beta(i-1)\Gamma(i)\mathbf{u}_k^H(i)\mathbf{f}(i-1)\mathbf{h}^H\mathbf{C}_k^H\mathbf{s}_k(i)). \quad (75)$$

Rewrite (34) as

$$\Gamma(i) = \beta(i-1)\mathbf{h}^H\mathbf{C}_k^H\mathbf{s}_k(i) + \beta(i-1)\Gamma(i)\mathbf{u}_k^H(i)\mathbf{f}(i-1)\mathbf{h}^H\mathbf{C}_k^H\mathbf{s}_k(i). \quad (76)$$

Comparing (75) and (76) we obtain (30).

E. Derivation of (37) and (38)

We have

$$\begin{aligned} \mathbf{Q}_k(i) &= \gamma(i)\mathbf{Q}_k(i-1) + \mathbf{u}_k(i)\mathbf{u}_k^H(i) \\ &= \mathbf{u}_k(i)\mathbf{u}_k^H(i) + \gamma(i)\mathbf{u}_k(i-1)\mathbf{u}_k^H(i-1) \\ &\quad + \gamma(i)\gamma(i-1)\mathbf{u}_k(i-2)\mathbf{u}_k^H(i-2) + \cdots + \gamma(i)\gamma(i-1)\cdots\gamma(2)\mathbf{u}_k(1)\mathbf{u}_k^H(1) \\ &\quad + \gamma(i)\gamma(i-1)\cdots\gamma(2)\gamma(1)\mathbf{u}_k(0)\mathbf{u}_k^H(0). \end{aligned} \quad (77)$$

For large i , there exists a number $N_i > 0$, when $i \geq N_i$, for which we have that the forgetting factor $\gamma(i)$ varies slowly around its mean value and $E[\gamma(N_i)] \approx E[\gamma(N_i+1)] \approx \cdots \approx E[\gamma(i)] \approx E[\gamma(\infty)]$.

By taking the expectation of (77) we obtain

$$\begin{aligned} E[\mathbf{Q}_k(i)] &\approx E[1 + \gamma(i) + \gamma(i)\gamma(i-1) + \cdots + \gamma(i)\gamma(i-1)\cdots\gamma(N_i)]E[\mathbf{u}_k(i)\mathbf{u}_k^H(i)] \\ &\quad + E[\gamma(i)\gamma(i-1)\cdots\gamma(N_i)]E[\gamma(N_i-1)\mathbf{u}_k(N_i-2)\mathbf{u}_k^H(N_i-2) + \cdots] \\ &\quad + \gamma(N_i-1)\gamma(N_i-2)\cdots\gamma(2)\gamma(1)\mathbf{u}_k(0)\mathbf{u}_k^H(0)] \\ &\approx (1 + E[\gamma(i)] + E^2[\gamma(i)] + \cdots + E^{i-N_i+1}[\gamma(i)])E[\mathbf{u}_k(i)\mathbf{u}_k^H(i)] + E^{i-N_i+1}[\gamma(i)]\Delta, \end{aligned} \quad (78)$$

where $\Delta = E[\gamma(N_i - 1)\mathbf{u}_k(N_i - 2)\mathbf{u}_k^H(N_i - 2) + \dots + \gamma(N_i - 1)\gamma(N_i - 2)\dots\gamma(2)\gamma(1)\mathbf{u}_k(0)\mathbf{u}_k^H(0)]$ is a constant matrix. Note that $0 < E[\gamma(i)] < 1$, when $i \rightarrow \infty$, we obtain

$$E[\mathbf{Q}_k(i)] \approx \frac{1}{1 - E[\gamma(\infty)]} E[\mathbf{u}_k(i)\mathbf{u}_k^H(i)]. \quad (79)$$

By adjusting the parameter ν to have the convexity of the CCM design [14], [15] and using the expressions of the adaptive CCM-RLS receiver (12)-(15), when $i \rightarrow \infty$, due to the fact that the time average approximates the statistical ensemble average, we have $E[\mathbf{u}_k(i)\mathbf{u}_k^H(i)] = \bar{\mathbf{Q}}_0$ and

$$\begin{aligned} E^{-1}[\mathbf{Q}_k(i)] &\approx (1 - E[\gamma(\infty)])\bar{\mathbf{Q}}_0^{-1} \\ &\approx (1 - E[\gamma(\infty)])E^{-1}[|z_0(i)|^2]\mathbf{R}^{-1}. \end{aligned} \quad (80)$$

Note that, when $i \rightarrow \infty$, $\mathbf{Q}_k(i)$ and $\mathbf{Q}_k^{-1}(i)$ converge. Thus, we assume $\lim_{i \rightarrow \infty} \mathbf{Q}_k^{-1}(i) \approx \lim_{i \rightarrow \infty} E[\mathbf{Q}_k^{-1}(i)] \approx \lim_{i \rightarrow \infty} E^{-1}[\mathbf{Q}_k(i)]$. Finally, we obtain (37).

By using the expression

$$\mathbf{d}_k(i) = \gamma(i)\mathbf{d}_k(i-1) + z_k^*(i)\mathbf{r}(i) \quad (81)$$

and following the same approach we can have (38).

REFERENCES

- [1] M. Honig, U. Madhow, and S. Verdú, "Blind adaptive multiuser detection," *IEEE Trans. Inf. Theory*, vol. 41, pp. 944-960, Jul. 1995.
- [2] Z. Xu and M. K. Tsatsanis, "Blind adaptive algorithms for minimum variance CDMA receivers," *IEEE Trans. Commun.*, vol. 49, no. 1, pp. 180-194, Jan. 2001.
- [3] R. C. de Lamare and R. Sampaio-Neto, "Low-Complexity Variable Step-Size Mechanisms for Stochastic Gradient Algorithms in Minimum Variance CDMA Receivers," *IEEE Trans. Signal Proc.*, vol. 54, no. 6, pp. 2302-2317, Jun. 2006.
- [4] A. El-Keyi and B. Champagne, "Adaptive Linearly Constrained Minimum Variance Beamforming for Multiuser Cooperative Relaying Using the Kalman Filter," *IEEE Trans. Wireless Commun.*, vol. 9, no. 2, pp. 641-651, Feb. 2010.
- [5] R. C. de Lamare, L. Wang, and R. Fa, "Adaptive reduced-rank LCMV beamforming algorithms based on joint iterative optimization of filters: Design and analysis," *Signal Processing*, vol. 90, pp. 640-652, Aug. 2009.
- [6] R. Fa, R. C. de Lamare and L. Wang, "Reduced-Rank STAP Schemes for Airborne Radar Based on Switched Joint Interpolation, Decimation and Filtering Algorithm" *IEEE Trans. Signal Proc.*, vol. 58, no. 8, pp. 4182-4194, Aug. 2010.
- [7] Z. Xu and P. Liu, "Code-constrained blind detection of CDMA signals in multipath channels," *IEEE Signal Process. Lett.*, vol. 9, pp. 389-392, Dec. 2002.
- [8] M. L. Honig and H. V. Poor, "Adaptive interference suppression," *Wireless Communications: Signal Processing Perspectives*. Englewood Cliffs, NJ: Prentice-Hall, 1998, ch. 2, pp. 64-128.
- [9] V. Krishnamurthy, "Averaged stochastic gradient algorithms for adaptive blind multiuser detection in DS/CDMA systems," *IEEE Trans. Commun.*, vol. 48, pp. 125-134, Feb. 2000.
- [10] D. Das and M. K. Varanasi, "Blind adaptive multiuser detection for cellular systems using stochastic approximation with averaging," *IEEE J. Sel. Areas Commun.*, vol. 20, no. 2, pp. 310-319, Feb. 2002.
- [11] P. Yuvapoositanon and J. Chambers, "An adaptive step-size code constrained minimum output energy receiver for nonstationary CDMA channels," in *IEEE Proc. Int. Conf. Acoust. Speech, Signal Process.*, Apr. 2003, vol. 4, pp. 465-468.

- [12] P. Yuvapoositanon and J. Chambers, "Adaptive step-size constant modulus algorithm for DS-CDMA receivers in nonstationary environments," *Signal Process.*, vol. 82, pp. 311-315, 2002.
- [13] Y. Cai and R. C. de Lamare, "Low-Complexity Variable Step-Size Mechanism for Code-Constrained Constant Modulus Stochastic Gradient Algorithms Applied to CDMA Interference Suppression," *IEEE Trans. Signal Proc.* vol. 57, no. 1, pp. 313-323, Jan. 2009.
- [14] R. C. de Lamare and R. Sampaio-Neto, "Blind Adaptive Code-Constrained Constant Modulus Algorithms for CDMA Interference Suppression in Multipath Channels," *IEEE Commun. Letters*, vol. 9, no. 4, pp. 334-336, Apr. 2005.
- [15] R. C. de Lamare, M. Haardt and R. Sampaio-Neto, "Blind Adaptive Constrained Reduced-Rank Parameter Estimation Based on Constant Modulus Design for CDMA Interference Suppression," *IEEE Trans. Signal Proc.* vol. 56, no. 6, pp. 2470-2482, Jun. 2008.
- [16] R. C. de Lamare, R. Sampaio-Neto and M. Haardt, "Blind Adaptive Constrained Constant-Modulus Reduced-Rank Interference Suppression Algorithms Based on Interpolation and Switched Decimation," *IEEE Trans. Signal Proc.* vol. 59, no. 2, pp. 681-695, Feb. 2011.
- [17] R. C. de Lamare and R. Sampaio-Neto, "Blind Adaptive and Iterative Algorithms for Decision-Feedback DS-CDMA Receivers in Frequency-Selective Channels," *IEEE Trans. vehicular Tech.*, vol. 56, no. 2, pp. 605-618, Mar. 2007.
- [18] R. C. de Lamare and R. Sampaio-Neto, "Blind adaptive decision feedback CDMA receivers for dispersive channels," *Electronics Letters*, vol. 40, no. 5, Mar. 2004.
- [19] T. Adali and S. H. Ardalani, "On the effect of input signal correlation on weight misadjustment in the RLS algorithm," *IEEE Trans. Signal Proc.*, vol. 43, no. 4, pp. 988-991, Apr. 1995.
- [20] E. Eleftheriou and D. D. Falconer, "Tracking properties and steady-state performance of RLS adaptive filter algorithms," *IEEE Trans. Acoust., Speech, Signal Processing*, vol. ASSP-34, pp. 1097-1109, Oct. 1986.
- [21] O. D. Macchi and N. J. Bershad, "Adaptive recovery of a chirped sinusoid in noise—Part I: Performance of the RLS algorithm," *IEEE Trans. Signal Proc.*, vol. 39, no. 4, pp. 583-594, Mar. 1991.
- [22] H. Zeng, L. Tong and C. R. Johnson, "Relationships Between the Constant Modulus and Wiener Receivers," *IEEE Trans. Inf. Theory*, vol. 44, no. 4, pp. 1523-1538, Jul. 1998.
- [23] R. Kwong and E. Johnston, "A variable step size LMS algorithm," *IEEE Trans. Signal Process.*, vol. 40, no. 7, pp. 1633-1642, Jul. 1992.
- [24] M. Gu and L. Tong, "Geometrical Characterizations of Constant Modulus Receivers," *IEEE Trans. Signal Proc.*, vol. 47, no. 10, pp. 2745-2756, Oct. 1999.
- [25] H. V. Poor and X. Wang, "Code-Aided Interference Suppression for DS/CDMA Communications-Part II: Parallel Blind Adaptive Implementations," *IEEE Trans. Commun.*, vol. 45, no. 9, pp. 1112-1122, Sep. 1997.
- [26] S. Haykin, "Adaptive Filter Theory," 4th ed. Englewood Cliffs, NJ: Prentice-Hall, 2002.
- [27] E. Eweda, "Comparison of RLS, LMS, and sign algorithms for tracking randomly time-varying channels," *IEEE Trans. Signal Process.*, vol. 42, pp. 2937-2944, Nov. 1994.
- [28] B. Widrow and S. D. Stearns, "Adaptive Signal Processing," Englewood Cliffs, NJ: Prentice-Hall, 1985.
- [29] C. Komninos, C. Fragouli, A. H. Sayed and R. D. Wesel, "Multi-Input Multi-Output Fading Channel Tracking and Equalization Using Kalman Estimation," *IEEE Trans. Signal Process.*, vol. 50, no. 5, pp. 1065-1076, May 2002.
- [30] X. G. Doukopoulos and G. V. Moustakides, "Adaptive Power Techniques for Blind Channel Estimation in CDMA Systems," *IEEE Trans. Signal Processing*, vol. 53, No. 3, pp. 1110-1120, March, 2005.
- [31] T. S. Rappaport, "Wireless Communications," Englewood Cliffs, NJ: Prentice-Hall, 1996.
- [32] J. B. Whitehead and F. Takawira, "Performance Analysis of the Linearly Constrained Constant Modulus Algorithm-Based Multiuser Detector," *IEEE Trans. Signal Processing*, vol. 53, No. 2, pp. 643-653, Feb., 2005.